Missile Guidance Laws
for a Strapdown Seeker
with a Narrow Field-of-View

좁은 화각을 갖는 스트랩다운 탐색기를 위한 유도기법

By

Chae Heun Lee

August 2013

SCHOOL OF ELECTRICAL ENGINEERING AND

COMPUTER SCIENCE

COLLEGE OF ENGINEERING

SEOUL NATIONAL UNIVERSITY

Missile Guidance Laws
for a Strapdown Seeker
with a Narrow Field-of-View

좁은 화각을 갖는 스트랩다운 탐색기를 위한 유도기법

지도교수 최 진 영

이 논문을 공학박사 학위논문으로 제출함

2013 년 8 월

서울대학교 대학원
전기공학부
이 채 흔

이채흔의 공학박사 학위논문을 인준함

2013 년 8 월

위 원 장 : _____

부위원장 : _____

위   원 : _____

위   원 : _____

위   원 : _____

Abstract
Missile Guidance Laws
for a Strapdown Seeker
with a Narrow Field-of-View

New guidance laws are proposed to solve the problem of when a missile is equipped with a strapdown seeker instead of a gimbaled seeker. The strapdown seeker has advantages of relatively simple implementation compared to a gimbaled seeker, and it can eliminate frictional cross-coupling significantly save on costs. There have been many studies to enable guided missiles to use strapdown seekers, but they have several weaknesses, such as measurement error caused by scale factor error, radome errors, glint noise, narrow field-of-view (FOV), and so on. Among these weak points, focus is centered on the narrow FOV of the strapdown seeker.

A hybrid guidance (HG) law is proposed to maintain the lock-on condition in spite of the narrow FOV of the strapdown seeker. The proposed HG law consists of two guidance phases, which assume operation at a switching boundary. In the first phase, the proportional navigation guidance (PNG) law is applied during the time when the

look angle is inside the switching boundary. For the second phase, when the look angle is outside the switching boundary, a new guidance law is derived to keep the look angle within the FOV by employing a Lyapunov-like function based on sliding-mode control methodology. The appropriate determination of the switching boundary is an important issue. The idea behind selecting the switching boundary is to use the PNG law as much as possible, and to make the missile stay in the lock-on condition.

A lock-on guidance (LOG) is proposed as another approach to solve the problem of narrow FOV, based on the concept of the pursuit guidance (PG) law. In order to derive the LOG law, we use a Lyapunov-like function based on the sliding-mode control methodology. An advantage of the LOG law is that a missile guided by the LOG law can intercept a target with a very narrow FOV of the strapdown seeker. Because such a seeker often has to be implemented for more accurate measurements, this kind of guidance law is needed to prepare for such a situation. The LOG law is simple and has good performance against a target with high speed.

Contents

List of Figures

List of Tables

Chapter 1

Introduction

1.1 Background and Motivations

Before World War II, there were many physical constraints under which a missile had to perform. In this period, it was more vital to design a proper propulsion system that could carry the missile, rather than to design a guidance system that could accurately intercept a target. However, at the end of World War II, missiles needed to be more accurate and more reliable. These demands produced the classical guidance laws, which were based on very simple ideas. These classical guidance laws advantages in that they are easy to understand, easy to implement, and needed simple information input. Because of this, classical guidance laws are adequate for use in present tactical missile systems. The classical guidance laws have been modified and improved through continuous research as follows [1]:

- Pursuit guidance laws - Derivations of pursuit guidance were provided by Locke and Howe, and in a review by Teng and Phipps [2-4]. Rishel and Goodstein [5, 6] compared the performance and sensitivity of pursuit guidance laws with several other standard guidance techniques.

- Line-of-sight guidance laws – Clemow [7] provided a detailed development of

BR and CLOS implementation. Harmon et al. [8] described a bang-bang approach to LOS guidance commands, while a pulse duration modulation scheme was explored for a wire-guided missile by Thibodeau and Sharp [9]. Ivanov [10] considered radar-based guidance methods and typical implementations of missile-borne seekers. Kain and Yost [11] employed a CLOS guidance scheme in a ship defense scenario, using optimal linear filters to reduce the inherent beam jitter.

- Proportional navigation guidance laws - Spits [12] derived the kinematic equations of a missile guided by a proportional navigation guidance (PNG). Irish [13] proposed a PNG scheme for a terminal rendezvous problem. McElhoe [14] showed that PNG can be used for a minimum-fuel intercept. Wong [15] gave a good overview of PNGs. Guelman [16] derived a closed-form solution of the pure PNG (PPNG) law for the case of a non-maneuvering target. Guelman [17] also showed via the phase-plane method that a missile guided by the PPNG law can always intercept a target maneuvering with constant normal acceleration. Ha et al. [18] proved via a Lyapunov-like method that a missile guided by the PPNG law can always intercept a target maneuvering randomly with time-varying normal acceleration. Ghose [19, 20] analytically obtained the capture regions for the true PNG (TPNG) and generalized TPNG (GTPNG) law, and proposed a method for obtaining the capture region of the GTPNG law. Yuan [21]

proposed an ideal PNG (IPNG) law and derived the closed-form solution for maneuvering and non-maneuvering targets.

After the 1960s, a movement towards using rigorous mathematical frameworks for these guidance laws began to emerge with the rapid developments in optimal control theory and its applications. Research on modern guidance laws began in this period.

- Optimal control guidance – Bryson et al. [22], Denham and Bryson [23], and Denham [24] were among the first to apply optimization techniques to missile guidance problems. Both Rang [25] and Rishel [26] considered linear missile models and minimized a quadratic form to achieve a guidance law using state feedback. Axelband and Hardy [27, 28] used linear optimal control to develop an extension of PNG.

- Game theory based guidance - Anderson [29] developed an iterative technique for the near optimum solution of a nonlinear differential game based on the successive linearization of a two-point boundary value problem. Pouler and Anderson [30] applied this scheme to an air-to-air missile guidance problem and reported much improved simulation results compared to a PNG law. Gupta and Sridhar [31] also proposed a guidance scheme based on reachable sets, in which a mapping of target acceleration capabilities into missile command acceleration

requirements was made. Gutman [32] considered a class of simple differential games in which the pursuer has first-order dynamics, and the evader has ideal dynamics.

- Predictive guidance - Best [33] presented a guidance framework based on model predictive control with the objective of maximizing the probability of successful interception. Dionne [34] presented a new terminal guidance law for pursuit-evasion problems with uncertain information about the target state employing the notion of a reachable set. The reachable set is restricted by the presence of hard actuation constraints.

- Sliding-mode control based guidance – Babu [35] proposed a new form of the PN guidance law for short-range homing missiles by invoking sliding-mode control theory. Zhou [36] proposed an adaptive sliding-mode guidance law which is robust against disturbances and parameter perturbations. Moon [37] proposed a missile guidance law utilizing sliding-mode control. This proposed guidance law does not need precise measurements of target acceleration, and uses the target acceleration bound instead.

The strapdown seeker has advantages such as significant cost savings, small size, and mechanical simplicity. However, the strapdown seeker has weak points in that the seeker measurements are error sources due to scale factor error, radome errors, glint

noise, and inherent angle alignment errors. The strapdown seeker also has other disadvantages, such as a limited, narrow field of view (FOV). So far, the strapdown seeker has only been used in the attached form of guidance modules on rockets such as the LCPK and APKWS (Fig 1.1). Much research has been conducted to address the weak points of the strapdown seeker.

Mehra and Ehrich [38] proposed an advanced guidance for short-range air-to-air BTT missiles using an active strapdown seeker. The seeker scale factor errors and low frequency glint were analyzed. Yun [39] proposed a guidance filter aided by an IMU, two magnetometers, a barometer, and a strapdown seeker. Du constructed a strapdown seeker scale factor error parasitical loop model, and analyzed the effect of the scale factor error on the effective navigation ratio. Kim [40] suggested a look angle control guidance, which controls the look angle measured by the strapdown seeker directly.

Figure 1.1: Application of a strapdown seeker

There has been much research on the parasite loop caused by the difference of the dynamics between the rate gyro and estimation of the look angle rate [41-47].

When using a strapdown seeker, the sensor cannot measure the line-of-sight (LOS) rate, which is used to generate an acceleration command. Much research has been done to estimate the line-of-sight rate of a strapdown imaging seeker based on filters such as an extended Kalman filter (EKF), unscented Kalman filer (UKF), and particle filter (PF) [48-50].

We focus here on the narrow FOV of the strapdown seeker among its several weak points. Xin et al. [51] used the seeker FOV as a constraint of a nonlinear optimal control problem to create a missile guidance law. Sang [52] proposed a guidance law switching logic between an original law such as PNG and a guidance law which makes the look angle constant during the homing phase at a predefined FOV limit. These two instances are limited to a target standing still. To overcome the limitation of FOV for a high-speed target, two new guidance laws are proposed: hybrid guidance (HG) law and lock-on guidance (LOG) law.

1.2   Contents of the Research

The goal is to enhance the guidance performance for when a strapdown seeker is mounted on a missile. The proposed guidance laws can be applied to engagements against a high-speed target using a strapdown seeker with a narrow FOV. The

contributions of the proposed guidance laws are:

Hybrid Guidance (HG) Law

・The HG law is developed for a missile on which a strapdown seeker with narrow FOV is mounted.

・The sliding-mode guidance (SMG) law for the second phase guidance is derived to reduce the look angle to zero, and to keep the look angle within the FOV by employing a Lyapunov-like function with sliding-mode control methodology.

・The switching boundary estimator is proposed to use the PNG law as much as possible and to maintain the lock-on condition.

・The HG law is designed by combining the SMG and PNG laws together with a switching boundary estimator for solving the problems with the narrow FOV of the strapdown seeker against a high speed target.

・The HG law solves the problem of a missile not being able to chase a target with conventional guidance laws due to the narrow FOV of the strapdwon seeker.

Lock-on Guidance Law

・The LOG law is proposed after considering a strapdown seeker which has an extremely narrow FOV against a high-speed target.

・The LOG law is derived using the concept of the PG law and a Lyapunov-like

function with sliding-mode control methodology.

・The LOG law shows satisfactory performance in both accuracy and reliability, and can be effectively applied to a missile with a strapdown seeker in air-to-air engagements.

Chapter 1 describes the backgrounds and motivations, as well as various research conducted.   Chapter 2 gives a preliminary survey. In section 2.1, guidance laws are classified into classical guidance laws and modern guidance laws. In sections 2.1.1 and 2.1.2, the classical guidance laws and modern guidance laws are explained in detail. Section 2.1.3 summarizes the conventional guidance for short-range tactical missiles. In section 2.2, the gimbal seeker and strapdown seeker are introduced and compared.

Chapter 3 presents the proposed guidance laws. Section 3.1 explains the hybrid guidance (HG) law. In section 3.1.1, the problem generated when the convention PNG law is applied to the strapdown seeker due to its narrow FOV is described, and the assumptions needed to derive the HG law are given. In section 3.1.2, the concept of the HG law is explained. The HG law consists of two guidances: a PNG law and an SMG law. The PNG law is explained in section 3.1.3, and the SMG law is derived in section 3.1.4. In section 3.1.5, the switching boundary estimation used to switch appropriately between the two guidance laws is explained. In section 3.2, we propose the lock-on guidance (LOG) law. Section 3.2.1 explains the relation between a seeker's accuracy

and FOV, which is the reason for proposing the LOG law, and shows the shortcomings of the HG law and the conventional law in the case that the FOV of the seeker is becoming narrower. In addition, the assumptions to derive the LOG law are provided. Section 3.2.2 addresses the problems of the PG law and the concept of the LOG law, which is based on the concept of the pursuit guidance (PG) law and makes up for the PG law's shortcomings. Section 3.2.3 presents the derivation of the LOG law.

Chapter 4 shows the simulation results of the proposed HG law and LOG law in order to verify their performance. Each proposed guidance law is simulated against non-maneuvering and maneuvering targets with high speed. Chapter 5 presents the conclusions and directions for further study.

Chapter 2

Preliminary Survey

2.1   Survey on Guidance Laws

The primary objective of the guidance subsystem in a tactical missile is to generate suitable commands so that the missile comes closer and closer to its target. In subsequent sections, we will briefly describe several classical and modern guidance laws for tactical missiles. The taxonomy of the various kinds of guidance laws for tactical missiles is given in Fig 2.1. In this figure, guidance laws have been sub-divided into classical guidance laws and modern guidance laws. In the following sections, we explain these classical and modern guidance laws in detail.

2.1.1 Classical Guidance Laws

Classical guidance laws are based on very simple ideas. These ideas are intuitively appealing, but do not have any theoretical basis, and are rather empirical. However, it is widely known that these classical guidance laws are optimal under some simplified assumptions. In the following sections, we introduce several classical guidance laws in detail.
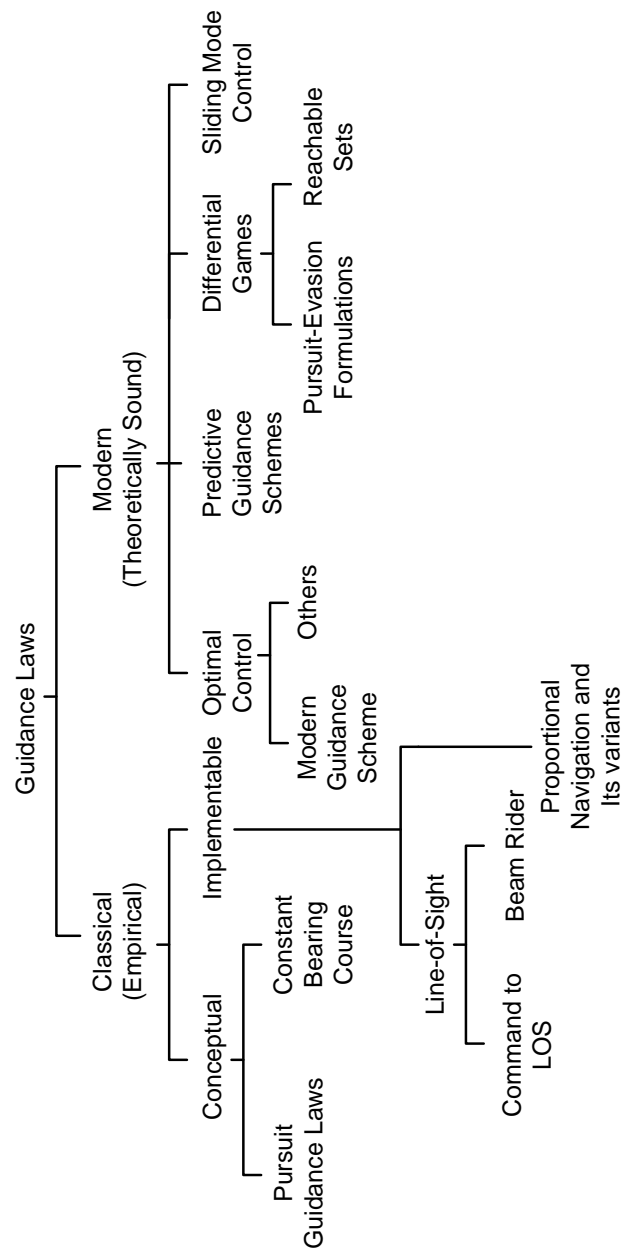
Figure 2.1 Taxonomy of conventional guidance laws.

2.1.1.1 Pursuit Guidance Law

Pursuit guidance law is not as effective as proportional navigation, but offers simpler mechanization advantages. In this guidance law, an attempt is made to keep the turning rate of the missile equal to the line-of-sight according to:

$$\dot{\gamma} = \dot{\sigma},$$

(2.1)

where γ is the missile flight path angle and σ is the line-of-sight angle. The turning rate of the missile is related to the missile acceleration a_m and velocity V_m. Since the acceleration command a_{mc} is equal to the lateral acceleration a_m, the pursuit guidance law can be expressed mathematically as:

$$a_{mc} = V_m \dot{\sigma}.$$

(2.2)

The pursuit guidance appears to be very similar to proportional navigation, except that the gain is unity rather than an effective navigation ratio.

The pursuit guidance has a problem in that the missile has to take a very sharp turn near the target. The next stage in the development of this guidance law addressed this problem, and was called the deviated pursuit guidance law. In the pursuit guidance law, the missile does not point toward the target, but at a point slightly ahead of it. This scheme reduces the demand on the guidance system in terms of the turn radius, but has other problems. One problem is the fact that if the target changes its direction of flight,

then the angular deviation must also change accordingly. The implementation of this is not a trivial matter.

Other variations of the pursuit guidance are the attitude pursuit and the velocity pursuit. In the attitude pursuit, the missile's centerline or the longitudinal axis is made to point toward the target, whereas in the velocity pursuit, the velocity vector of the missile is made to point toward the target. These two are different, since the velocity vector of a missile lags its longitudinal axis by the angle-of-attack.

2.1.1.2 Constant Bearing Course Guidance Law

All guidance laws actually try to achieve the performance of the constant bearing course guidance law, which is conceptually the best guidance law. Fig 2.2 shows the collision triangle. The collision triangle satisfies:

$$V_m \sin \theta_m = V_t \sin \theta_t.$$

(2.3)

When the missile flies along $\overline{MC}$, we can say that the missile is on a collision course.

2.1.1.3 Line-of-Sight Guidance Law

The basic idea behind the line-of-sight (LOS) guidance law is that the missile follows the line-of-sight from the launch station to the target at any given instant in time. The LOS guidance law can be divided into two types according to the
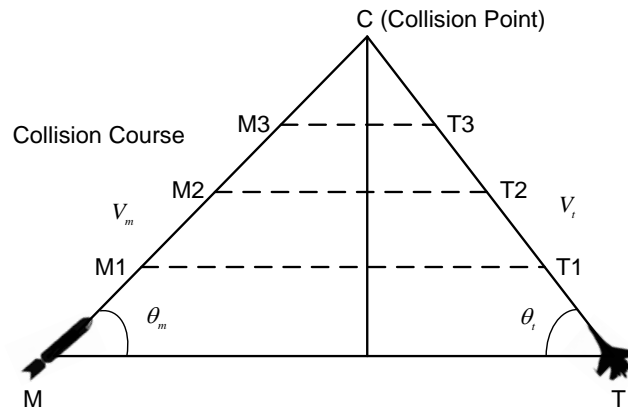
Figure 2.2 Collision triangle.

mechanization of the missiles.

Command-to-Line-of-Sight (CLOS) Guidance law

The command-to-line-of-sight (CLOS) guidance law is a missile control policy designed to achieve an intercept between a missile and a desired target by forcing the missile to fly along the instantaneous line-of-sight between an external tracker and the target. The corresponding instantaneous geometry is illustrated in Fig 2.3.

Beam Rider (BR) Guidance Law

The concept of the beam rider is presented in Fig 2.4. The missile guidance system inside the missile senses the deviation of the missile position from the beam, and generates guidance commands to enable the missile to stay inside the beam. The beam may be a radar beam or a laser beam, and the source of the beam is attached to the
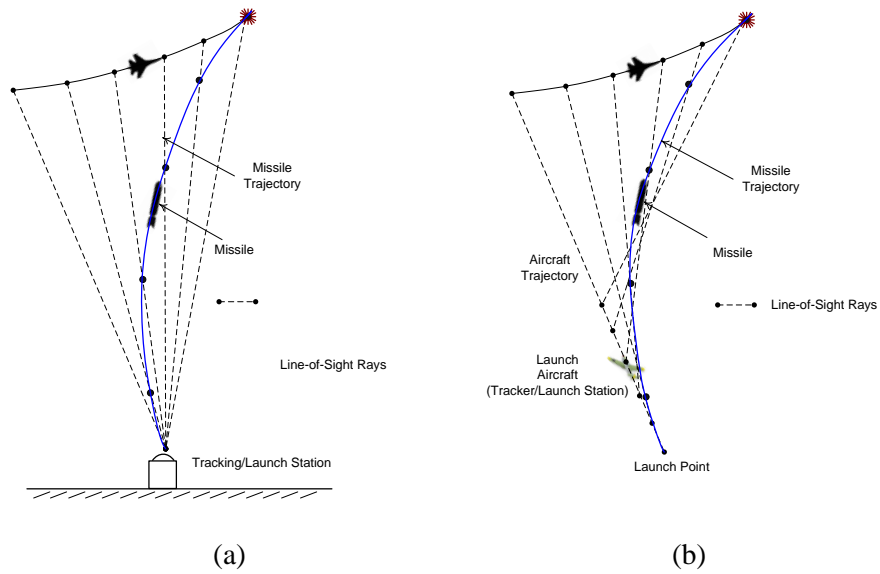
Figure 2.3: Typical CLOS guidance trajectories for a missile, a target, and (a) a ground tracking/launch station or (b) a launch aircraft.
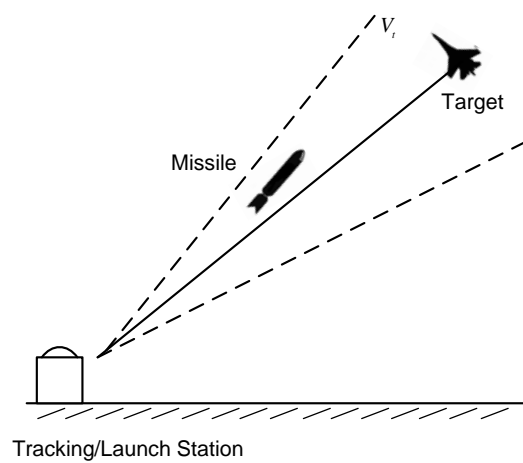
Figure 2.4: Concept of beam-rider guidance.

launcher itself. The missile receives the beam signal, which helps the missile determine how far from the beam axis the missile is. The Talos beam-rider missile is an example of an early missile that uses this principle.

2.1.1.4 Proportional Navigation Guidance Law

The proportional navigation guidance (PNG) law is the most important guidance law of all the classical guidance laws, and applies the principle of the constant bearing guidance in the most logical way. The PNG is the most widely used law in practice. The concept of the PNG is that missile acceleration should nullify the line-of-sight (LOS) rate between the target and the missile. According to the principle of the constant bearing guidance, the LOS rate must be equal to zero. In reality, it differs from zero, so that the guidance command that is proportional to the rate of the LOS change may decrease the absolute value of the LOS rate, and it will tend to be closer to zero. A guidance command ensures that the rate of rotation of the missile velocity vector is proportional to the rate of the LOS as:

$$\dot{\gamma}_m = N\sigma,$$

(2.4)

where N is the navigation constant.

Pure Proportional Navigation Guidance Law

The lateral acceleration by the pure PNG (PPNG) law is applied normal to the

velocity vector of the missile. The engagement geometry in the PPNG law is depicted

in Fig 2. 5. The target moves with the velocity V_t and the normal acceleration a_t.

The missile chases the target with the velocity V_m and the normal acceleration a_m.

The strapdown seeker measures the look angle θ_m, which depends on the attitude of

the missile and the LOS angle σ. The LOS angle used in the PPNG law is obtained

by combining the look angle and the attitude of the missile.

Based on the engagement geometry of Fig 2.5, the kinematics and the dynamics are

obtained as follows:

$$\dot{\gamma}_t = \frac{a_t}{V_t}, \tag{2.5}$$

$$\dot{\gamma}_m = \frac{a_m}{V_m}, \tag{2.6}$$
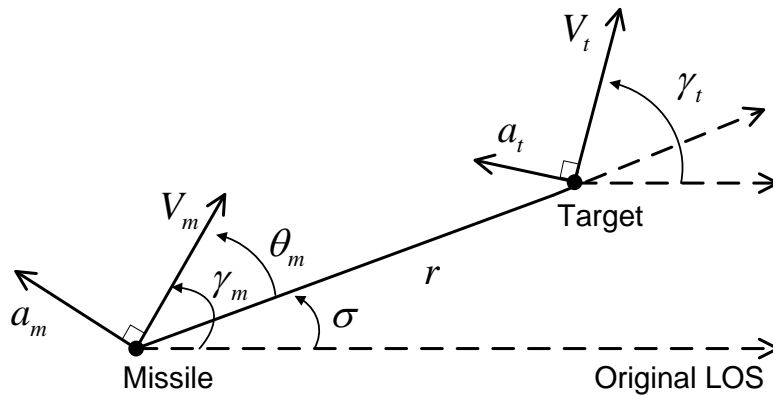
Figure 2.5: Geometry of PPNG law.

$$\dot{r} = V_t \cos\theta_t - V_m \cos\theta_m, \tag{2.7}$$

$$r\dot{\sigma} = V_t \sin\theta_t - V_m \sin\theta_m, \tag{2.8}$$

where θ_t, θ_m, and a_{mc} are defined by:

$$\theta_t = \gamma_t - \sigma, \tag{2.9}$$

$$\theta_m = \gamma_m - \sigma, \tag{2.10}$$

where γ_t is a target flight angle.

The PPNG law can be defined by:

$$a_{mc} = NV_m \dot{\sigma}. \tag{2.11}$$

Eq. (2.6) is valid when the lateral acceleration a_m is perpendicular to the missile velocity V_m. If we ignore the angle-of-attack of the missile, then this direction of the acceleration command is the natural direction of the lateral force.

<u>True Proportional Navigation Guidance Law</u>

The velocity of interest is actually the closing velocity, because the LOS rate is derived to be zero. The difference between the PPNG law and the true PNG (TPNG) law is that the desired lateral acceleration by the TPNG law is applied normal to the instantaneous LOS, not to the missile velocity. Fig 2.6 presents the engagement

geometry for when the missile is guided by the TPNG law. The equations of motion in

the TPNG law case are:

$$\dot{V}_m = a_m \sin\theta_m, \tag{2.12}$$

$$\dot{\gamma}_m = \frac{a_m \cos\theta_m}{V_m}, \tag{2.13}$$

$$\dot{r} = V_t \cos\theta_t - V_m \cos\theta_m, \tag{2.14}$$

$$r\dot{\sigma} = V_t \sin\theta_t - V_m \sin\theta_m. \tag{2.15}$$

The TPNG law can be derived as:

$$a_m = N'V_c\dot{\sigma}, \tag{2.16}$$

where N' is the effective navigation ratio, and V_c is the closing velocity. A

significant problem of the TPNG law is the implementation, since the direction of the

applied lateral acceleration is not a natural direction of the lifting force generated by
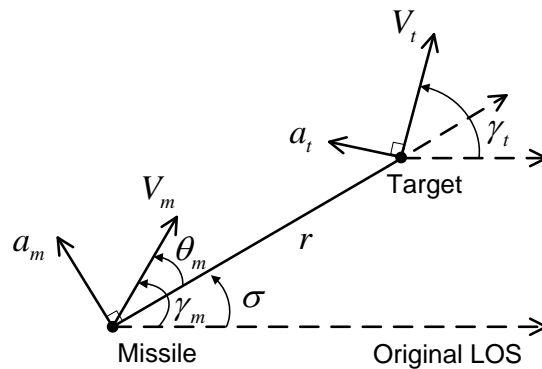
Figure 2.6: Geometry of TPNG law.

the missile airframe. So, this guidance law needs additional thrusters in order to impart

an additional longitudinal acceleration. The extra additional thrusters make the TPNG

law unsuitable as a practical solution.

Generalized True Proportional Navigation Guidance Law

The idea behind the generalized true proportional navigation guidance is to increase

the capturability performance of the guidance law further, and to make it comparable to

the PPNG law. Fig 2.7 depicts the engagement geometry for when the missile is guided

by the Generalized TPNG (GTPNG) law. In the RTPNG law, the commanded lateral

acceleration is applied at any arbitrary angle instead of normal to the LOS.

According to the TPNG law, the missile acceleration applied in a direction normal to

the LOS is:

$$a_m = c\dot{\sigma},$$
(2.17)

where c is a constant. In the RTPNG law, the lateral acceleration a_m is composed of

the acceleration along the LOS a_{mr} and the acceleration normal to LOS $a_{m\sigma}$. Then,

we have:

$$a_{mr} = a_m \sin\eta,$$
(2.18)

$$a_{m\sigma} = a_m \cos\eta,$$
(2.19)

where η is the angle between the arbitrary acceleration vector and the acceleration
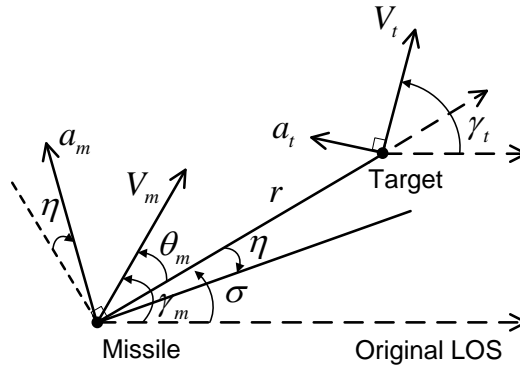
Figure 2.7: Geometry of GTPNG law.

normal to the LOS. Analogous to Eq. (2.17), we define:

$$a_{m\sigma} = c_1 \dot{\sigma}, \qquad a_{mr} = c_2 \dot{\sigma}. \qquad (2.20)$$

Then,

$$c = \left(c_1^2 + c_2^2 \right)^{1/2}, \qquad (2.21)$$

where $c_1 = c \cos \eta$, and $c_2 = c \sin \eta$. The signs of c_1 and c_2 depend on η.

Ideal Proportional Navigation Guidance Law

A further significant development in this direction occurred when another variant of the PNG law called the ideal PNG (IPNG) law was proposed. The commanded lateral acceleration was applied perpendicular to the relative velocity between the missile and the target. It is easy to see that the arguments of the IPNG law are similar to the arguments of the TPNG law. However, the performance differed significantly. It was

found that the capturability of this law was comparable to that of the PPNG law, and

much better than that of the TPN law or its many generalizations. The problem of the

IPNG law is that the IPNG law is as difficult to implement as the TPNG law or any of

its generalizations.

Consider the missile with velocity $\vec{v}_m$ pursuing a non-maneuvering target with

velocity $\vec{v}_t$ in the same plane under the IPNG law. We define the relative velocity $\vec{v}$

between the missile and the target as:

$$
\begin{aligned}
\vec{v} &= \vec{v}_m - \vec{v}_t \\
&= v_r \vec{e}_r + v_\sigma \vec{e}_s \\
&= \dot{r} \vec{e}_r + r \dot{\sigma} \vec{e}_s.
\end{aligned}
\tag{2.22}
$$

As shown in Fig 2.8, the lateral acceleration command is applied normal to the

relative velocity $\vec{v}$, and its magnitude is proportional to the product of the LOS rate

and the relative velocity as:
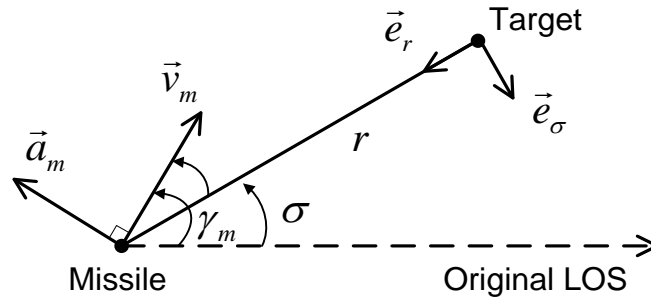
Figure 2.8: Geometry of IPNG law.

$$a_c = \lambda \dot{\sigma} e_z \times \vec{v}$$
$$= \lambda \left(-r\dot{\sigma}^2 \vec{e}_r + \dot{r}\dot{\sigma}\vec{e}_\sigma \right). \tag{2.23}$$

where $e_z = \vec{e}_r \times \vec{e}_\sigma$.

2.1.2 Modern Guidance Laws

Modern guidance laws were developed by the application of optimal control theory to missile guidance problems. In these laws, the kinematic equations for the missile and target engagement are considered as a state-space model of a dynamical system. The guidance problem is formulated in many different ways, depending on the requirements of the mission. The performance criteria are the minimization of the miss distance, integral square control effort, and guidance time. Another requirement can be a constraint on the lateral acceleration. Most of these problems have no closed-form solution, since the kinematic equations are highly non-linear. This makes the guidance laws derived by this method complicated. These guidance laws have very complicated two-point boundary value problems, which were solved with great difficulty due to the sensitivity of the terminal conditions with respect to the initial conditions on the Lagrange multipliers or co-state variables. Even if it is possible to solve these problems, much time is required to compute the exact guidance command. This is unacceptable, as these guidance laws either have to be implemented on-board on microprocessors, or solved by portable minicomputers.

2.1.2.1 Optimal-Control-Based Guidance Law

Guidance based on optimal control is obtained from a linearized geometry. The linearization of the missile and target geometry can easily be accomplished if we define some new relative quantities, as shown in Fig 2.9. In this figure, y is the vertical separation between the missile and the target. Under the assumption that the autopilot has first-order dynamics, the state equation of this engagement is:

$$\ddot{y} = a_t - a_m, \tag{2.24}$$

$$\dot{a}_m = -\frac{1}{\tau} a_m + \frac{1}{\tau} a_{mc}, \tag{2.25}$$

where τ is the time constant of the autopilot, a_{mc} is the lateral acceleration command, a_m is the achieved lateral acceleration perpendicular to the LOS of the missile and the target, and a_t is the acceleration of the target normal to the LOS.
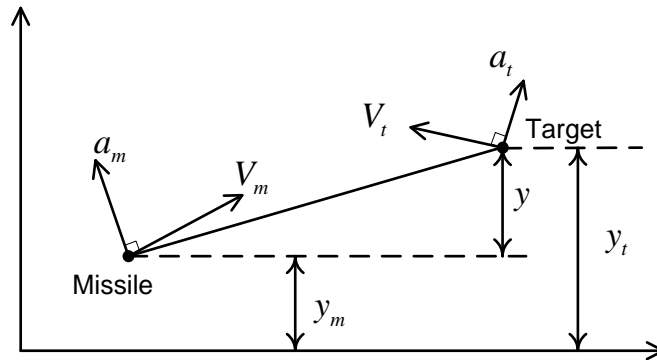
Figure 2.9: Geometry for linearization.

The integral square control effort is considered as the performance index. The minimization of the integral square control effort is meant to save fuel and minimize the maneuver-induced drag. The performance criterion is:

$$Minimize \int_0^{t_f} a_{mc}^2 dt.$$
(2.26)

This is subject to the terminal constraint $y(t_f)=0$, where t_f is the specified final time. This law can be written as:

$$a_{mc} = \frac{N'}{t_{go}^2}\left[y + \dot{y}t_{go} + \frac{1}{2}a_t t_{go}^2 - a_m(e^{-T} - 1 + T)\right],$$
(2.27)

where

$$t_{go} = t_f - t,$$
(2.28)

$$T = \frac{t_{go}}{\tau},$$
(2.29)

$$N' = \frac{6T^2(e^{-T} - 1 + T)}{2T^3 + 3 + 6T - 6T^2 - 12Te^{-T} - 3e^{-2T}}.$$
(2.30)

The effective navigation ratio N' is time-varying. In Eq. (2.30), when the time-to-go t_{go} is large or the time constant of the autopilot is small (corresponding to high bandwidth), the effective navigation ratio goes to 3.

The commanded acceleration by TPNG law is:

$$a_m = N'V_c\dot{\sigma}.$$
(2.31)

In the linearized geometry, the LOS rate $\dot{\sigma}$ is:

$$
\begin{aligned}
\dot{\sigma} &= \frac{d}{dt}\sigma \\
&= \frac{d}{dt}\frac{y}{R_{tm}} \\
&= \frac{y}{V_c t_{go}^2} + \frac{\dot{y}}{V_c t_{go}}.
\end{aligned}
\tag{2.32}
$$

Substituting Eq. (2.32) into Eq. (2.31), the acceleration command normal to the LOS becomes:

$$
a_m = \left(\frac{N'}{t_{go}^2}\right)\left(y + \dot{y}t_{go}\right).
\tag{2.33}
$$

Eq. (2.27) can be represented in another form:

$$
a_{mc} = \frac{N'}{t_{go}^2}(y + \dot{y}t_{go}) + \frac{N'}{2}a_t - N'a_m\left(\frac{e^{-T} - 1 + T}{t_{go}^2}\right).
\tag{2.34}
$$

Eq. (2.34) consists of three terms: a PN component, a target maneuver component, and an autopilot lag component. If the autopilot lag is ignored, the third term is eliminated, and Eq. (2.34) becomes the augmented proportional navigation guidance (APNG) law. When the autopilot is ideal, this law is optimal against a maneuvering target. In addition, if the target does not maneuver, this law becomes the general PNG law, which is optimal with $N'=3$.

The contribution of the modern guidance scheme is to show that the classical PNG law has a very strong theoretical justification. This has an advantage in that it is able to extend a number of other guidance laws. Important among them is the APNG law. This is optimal when the target maneuvers, and the autopilot of the missile is ideal.

The main disadvantage of the modern guidance scheme is non-implementability. The scheme requires not only an accurate estimate of the maneuvering target, but an accurate estimate of the time-to-go. In addition, for the purpose of implementing the component by the autopilot lag, this guidance law requires knowledge of the current maneuver level of the missile, which is a difficult quantity to measure. The MGS law requires an extra formation, such as the target acceleration, time-to-go, and the current missile acceleration.

2.1.2.2 Predictive Guidance Law

If an exact model of the target and missile dynamics were available, one could achieve the best performance with the predictive guidance law. The principle behind the predictive guidance law is quite simple. The predictive guidance law predicts the future position of the target based on the dynamic models of the target, and makes the best guidance strategy to intercept the target.

Consider a simplified linearized problem in the plane represented in the form of a stochastic linear system with continuous-time dynamics and with discrete-time measurements received at a given frequency $1/\Delta$:

$$\dot{x}_m(t) = A_m(t)x_m(t) + B_m(t)u(t), \tag{2.35}$$

$$\dot{x}_t(t) = A_t(t)x_t(t) + B_t(t)a(t), \tag{2.36}$$

$$y(t_k) = H(t_k)x_t(t_k) + v(t_k), \qquad t_k \triangleq k\Delta, \tag{2.37}$$

where $k = 0, 1, \cdots,$ and with $x_m(t) \in \mathbb{R}^{i_p}$, $x_m(t) \in \mathbb{R}^{i_E}$, $u(t) \in \mathbb{R}^1$, $a(t) \in \mathbb{R}^1$, and $y(t_k) \in \mathbb{R}^{i_y}$. The vectors x_m and x_t denote the states of the missile and the target, respectively. The measurement noise v is assumed to be normally distributed as $v \sim \mathrm{N}(o, Q_\eta)$. The signal u is assumed to be the acceleration command of the missile, and the signal a is an unknown signal representing the target's acceleration command.

Let the first component of the state vectors be denoted as $x_m^1 \in \mathbb{R}^1$ and $x_t^1 \in \mathbb{R}^1$. Let each represent the lateral position of the missile and of the target in the inertial reference frame of the missile. The objective of the guidance is to guide the pursuer so as to achieve $x_m^1(t_f) = x_t^1(t_f)$, where t_f is the intercept time.

Fig 2.10 presents a flow diagram of conventional predictive guidance. In this flow diagram, the notations mean as $z_t \triangleq x_t^1(t_f)$, y^k is the σ-algebra generated by the measurements: $y^k \triangleq \sigma\{y(t_s) : 0 < s \leq k\}$, and $p(z_m \mid y^k)$ is the conditional probability density function for the predicted position of the missile at the interception time.
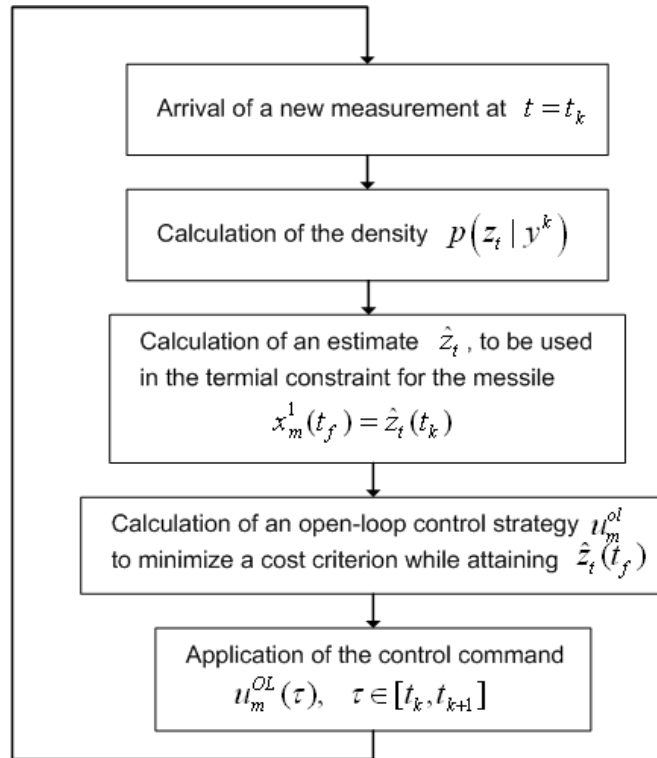
Figure 2.10: Flow diagram of predictive guidance law.

2.1.2.3 Game-Theory-Based Guidance Law

A pursuit-evasion game is used to consider how to guide one or more pursuers to catch one or more moving evaders. In the game theory, a game consists of three parts: players, actions, and lost functions. The solutions to a game are normally the policies for the players. With these policies, an equilibrium state will be achieved, and the players will have no regrets [53]. Each player tries to minimize his own performance index [54, 55]. The methods to solve the pursuit-evasion problems involve three approaches: one for problems with differential motion models, one using the worst-

case analysis, and one using probabilistic analysis.

If motion models of the players in the pursuit-evasion game are differential equations, then the game is called a differential game. The objective of a differential game is to find the saddle-point equilibria with respect to the game policy. In the worst-case analysis, it is assumed that only the game environment is known to the pursuers, and the evaders work as nature, which knows all information, such as the location of the pursuers, the environment, and even the policy of the pursuers. In the probabilistic analysis, the evaders are considered not to be superior to the pursuers, which might only have limited range and uncertain sensors, and it is also assumed that they do not know the environment.

The modern approach to missile guidance is based on optimal control theory and differential games. While the optimal control theory involves one-sided optimization of the optimization of the missile parameters, the differential games involve two-sided optimization of both the missile and the target parameters [56]. According to comparison studies based on extensive simulations, the interceptor guidance laws derived from a differential game formulation are superior to those obtained using optimal control theory. In spite of the results of these comparisons, the differential game guidance laws have not yet been adopted by the missile industry. This conservative attitude can be explained by the fact that the existing interceptor missiles have a sufficient maneuverability advantage over the presumed targets, even with the

simple but efficient conventional guidance laws. Moreover, applying the optimal pursuer strategy of the perfect information game as the guidance law of the interceptor using a typical estimator yields very disappointing results. The miss distance is never zero, and there is a high sensitivity to the structure of the unknown target maneuvers [57].

2.1.2.4 Sliding-Mode-Control-Based Guidance Law

The sliding-mode control (SMC) is one of the significant research topics in the control engineering domain. A number of important applications of the theory in fields such as power electronics, motion control, robotics, and bioprocess have been reported [58~66].

Utkin [67] introduced the Variable Structure Control (VSC) theory. Decarlo [68] presented the design of the VSC systems for a class of multivariable nonlinear time-varying systems. The design of the VSC has two steps. The first is to design the switching surface to assure the desired behavior of the plant in a sliding mode, and the second step is to develop the control law which forces the system's trajectory to a sliding surface and maintains it there.

SMC is based on VSC theory. B. Hamel initiated studies of SMC for nonlinear compensators. The main advantages of SMC are: 1) its robustness against a large class of perturbations or model uncertainties, 2) the need for a reduced amount of information in comparison to classical control techniques, 3) the possibility of

stabilizing some nonlinear systems which are not stabilizable by continuous-state feedback laws [69]. A main disadvantage of the SMC method is a phenomenon called chattering, because of the signum functions that are involved [70]. Many analytical design methods were proposed to reduce the effects of chattering [71-75].

In the guidance field, SMC has been proposed in the form of sliding mode guidance (SMG) law. Considering the missile-target engagement kinematics and choosing the relative position components as the state variables, the SMG laws are derived on the sliding surface of the zero LOS angular rate based on the Lyapunov method [35-37], [76]. We also use the sliding-mode control (SMC) in order to derive the proposed guidance laws.

2.1.3 Summary

Pastrick and Seltzer compared various guidance laws [77]. Table 2.1 depicts the comparison of various guidance concepts for short-range tactical missiles. The CLOS and BR concepts have extra ground stations, which have complex mechanizations. Their airframe complexity is relatively low and less expensive. The PNG is favorable for targets which are either stationary or moving with a constant velocity. The PNG is simple and relatively easy to implement. For highly maneuverable accelerating targets, optimal guidance laws are superior in guidance performance compared to the other approaches, but the microprocessor has extra requirements due to the vastly more complex computation.

Table 2.1 Comparison of conventional guidance laws for tactical missiles [77]

		Line-of-sight		Pursuit Guidance	PNG	Optimal Guidance
		CLOS	Beam-rider			
Ability to engage targets	Accuracy (ft CEP)	<2	<2	>30	<5	<1
	Maneuverability	Low	Low	Low	Const velocity	Accelerating
Gimbal mechanization (seeker)		No	No	No or Air vane	Gyro	Gyro
Cost(on-board)		0.8	0.9	1.0	1.6	1.8
Sensor requirements		Wire link	Optical link	Seeker	Seeker	Seeker (states measured and estimated)
Airframe/propulsion requirements		Low	Low	High	Low	High
Tactical considerations	Fire and	No	No	Possible	Possible	Possible
	Quick reaction time	No	No	Yes	Yes	Yes

2.2 Survey on Missile Seekers

Missile seekers can be classified into two types according to the way they are mounted on a missile. One is a gimbal type, in which the seeker is mounted on a platform that is stabilized by a gimbal system. Thus, the LOS angle and LOS angular rate, which are independent of the missile motion, can be directly measured. The other

is a strapdown type, in which the seeker is directly fixed to the missile body. So, the look angle measurement of seeker is affected by missile motion. Each type has relative advantages and disadvantages [78].

2.2.1 Gimbal Seeker

The gimbal seeker is more conventional. The seeker is mounted on a platform which is stabilized by complicated electronics and mechanical devices, such as servo motors and gyro sensors, and the gimbal seeker is independent of the motion of the missile. Because of the independence of the gimbal seeker and the missile body, the gimbal seeker can obtain continuous and directed measurements. Since these characteristics of the gimbal seeker are great advantages in a guidance system, the gimbal seeker is used in most guided missiles. However, the complex structure of the gimbal seeker increases the cost of implementing the seeker modules of the missile. The general seeker angular
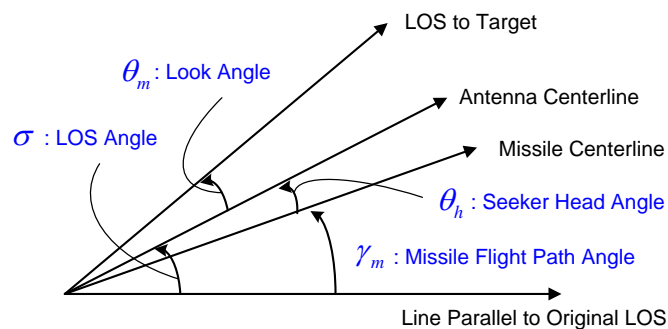
Figure 2.11: Angular configuration of a gimbal seeker.

configuration is depicted in Fig 2.11. In the gimbaled seeker, the antenna centerline and missile centerline move independently of each other by means of a seeker stabilization loop. The seeker head angle $\theta_h(t)$ can be varied.

2.2.2 Strapdown Seeker

The strapdown seeker is directly mounted on the missile body without the independently moving platform. Because the strapdown seeker is implemented without the platform, the cost of implementation is relatively low. In the strapdown seeker, the antenna centerline and missile centerline are fixed, because the strapdown seeker is rigidly mounted on the missile body. Therefore, their measurements are relative to the body frame of the missile. The strapdown seeker angular configuration is depicted in Fig 2.12. The antenna centerline of the strapdown seeker is aligned with the missile centerline, unlike with the gimbal seeker, meaning that $\theta_h = 0$.
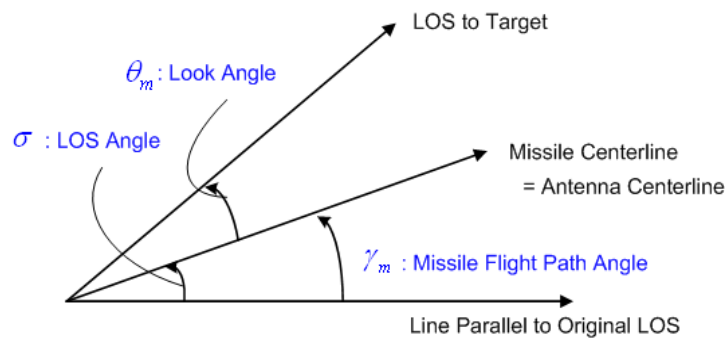
Figure 2.12: Angular configuration of a strapdown seeker

2.2.3 Summary

The missile requires a high kill probability when employed against a wide variety of highly maneuverable, intelligent targets. For this reason, the gimbal seeker is typically used in various kinds of the tactical missiles. However, the gimbal seeker is expensive, and is subject to the structural limitations of the stabilized gimbal platform. Also, the implementation and calibration of the gimbal seeker are mechanically complex. These mechanical parts cause frictional cross-coupling between the pitch and yaw tracking channels, and accuracy degradation due to the missile acceleration.

The strapdown seeker has potential for eliminating the disadvantages of the gimbal seeker due to the lack of the mechanical moving parts of the gimbal platform, enabling significant cost savings. Despite these advantages, the strapdown seeker has critical hazards associated when applying it to a guidance system. In the strapdown seeker, the seeker measurements are sources of error, which are contributed by scale factor error, random errors, glint noise, and inherent angle alignment errors. Another disadvantage is that the missile guidance requires inertial reference measurements, but the strapdown seeker only provides body-fixed measurements. Finally, the conventional guidance requires a large FOV to maintain lock-on condition, but the strapdown seeker has a narrow FOV [78, 79].

In Table 2.2, the comparison of the gimbal and strapdown seeker is summarized. We focus on the weak point related to the reduced FOV of the strapdown seeker.

Table 2.2 Comparison of the gimbal seeker and the strapdown seeker [78]

	Gimbal Seeker	Strapdown Seeker
Mounting	Mounted on a two-gimbal platform.	Rigidly mounted on the missile's body, doing away with a gimbaled platform.
FOV	Up to ±90 [deg]	About ±15 [deg]
Angle and Rate Measurements	LOS angle and LOS angular rate error angles w.r.t. the global frame.	LOS angle between the missile centerline and the LOS
Guidance Law Utilization	PNG can be easily implemented due to the LOS rate measurement.	PNG cannot be applied easily.
Measurement Results	Independent of the missile motion.	Dependent of the missile motion.
Major Sources of Measurement Errors	Gyro drift, gimbal friction, gimbal cross-couplings, radome refraction and acceleration sensitivity.	Glint noise and inherent angle alignment errors.
Cost	Higher than strapdown seeker due to the gimbal platform.	Low due to except the gimbal platform.

2.3 Remarks and Discussions

The guidance laws are classified into classical and modern guidance laws. The pursuit guidance, CLOS, beam-rider, and PNG laws are classical guidance laws. These guidance concepts are simple and easy to implement. However, the CLOS and beam-rider laws require extra complex ground or air stations to obtain LOS information. The pursuit guidance is suitable for a target that moves slowly. If the target has high speed, the missile must take a sharp turn near the target. The unreasonable maneuvering

required in the missile leads to an intercept performance. The PNG law is the most important guidance law of all the classical guidance laws, and is the most widely used law in practice. Among these guidance laws, both PPNG and TPNG are important. PPN makes the assumption that the angle-of-attack is zero, which is seldom the case. So, the actual PNG law is something that lies between the PPNG and TPNG.

The PNG has good guidance performance for targets which are either stationary or moving with a constant velocity, but the modern guidance laws are better for the maneuvering target. The modern guidance laws have been developed by the application of optimal control theory to missile guidance problems. These laws include guidance schemes based on optimal control, predictive guidance schemes, differential games, and guidance based on sliding-mode control. The classical PNG law has very strong theoretical justification. For highly maneuverable targets, these guidance laws have very good guidance performance. However, the microprocessor requires extra computation power due to the vastly more complex computation, and needs the extra information such as the target acceleration and time-to-go.

Next, two types of seekers, the gimbal and strapdown seeker, have been introduced. The gimbal has an advantage in that the gimbal seeker can obtain continuously directed measures such as the LOS rate, and more information such as the range between the missile and the target, as well as the closing velocity, because the seeker can stare directly at the target due to the independent motion of the gimbal seeker against the

missile body. However, the implementation and calibration of the gimbal seeker are mechanically complex. These mechanical parts would cause frictional cross-coupling between the pitch and yaw tracking channels, and accuracy degradation due to the missile acceleration. Above all, the implementation of the gimbal seeker is expensive. The strapdown seeker is an alternative solution, but there are several weak points. Among the weak points of the strapdown seeker, we concentrate on the narrow field-of-view (FOV).

Chapter 3

The Proposed Guidance Laws

3.1   Hybrid Guidance Law

This chapter proposes a new guidance law, which considers the Field of View (FOV) of the seeker when the missile mounts the strapdown seeker instead of the gimbal seeker. The FOV of the seeker is an important factor of guidance performance such as for the miss distance when the strapdown seeker - a narrow FOV - is used in the tracking target. A new guidance law, called the hybrid guidance (HG) law, is proposed because the conventional guidance law such as the proportional navigation guidance (PNG) law cannot maintain a lock-on condition against high speed targets due to the narrow FOV of the strapdown seeker. The aim of the HG law is to null the miss distance and to maintain look angle within the FOV of the strapdown seeker. In order to achieve this goal, we combine two guidance laws within the HG law. The first is a PNG law used to null the LOS rate and the second is a sliding mode guidance law derived to maintain the look angle within the FOV by employing a Lyapunov-like function with the sliding mode control methodology. We also propose a method to switch these two guidance law at a certain look angle for better guidance performance.

Xin, Balakrishnan and Ohlmeyer used the seeker FOV as a constraint of the nonlinear optimal control problem for solving the missile guidance law [48]. Daekyu

Sang proposed a guidance law with a switching logic between an original law (such as a PNG law) and an alternative guidance law, which makes the look angle constant during the homing phase at a predefined FOV limit [49]. However, these proposals are limited to motionless targets. Meanwhile, to overcome the limitation of FOV for a target which moves at high speed, this chapter proposes a hybrid guidance (HG) law. To maintain a lock-on condition, we proposed the HG law which combines two guidance laws: the first is a conventional PNG law used to null the LOS rate, while the second is a sliding-mode guidance (SMG) law, derived here to decrease the look angle of the strapdown seeker. The PNG law is used when the look angle is less than a certain angle (called a switching boundary) which represents the warning that the look angle may become larger than the FOV limit. The SMG law is used over the switching boundary. The switching boundaries are derived by considering guidance system characteristics such as time constant, the missile velocity, and the look angle rate. In this way, we increase the confidence in intercept success because the missile maintains the lock-on condition until a nearby target is reached.

3.1.1 Problem Statement

In order to show the problem when the conventional PNG law is applied to the strapdown seeker, we carried out the guidance simulation of the PNG in a specific engagement situation. Fig 3.1 shows the simulation result supposing that the missile

(a)   (b)
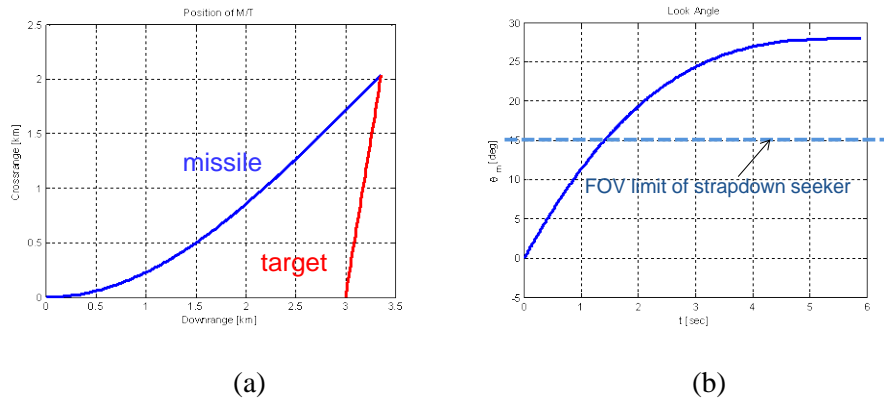
Figure 3.1: Simulation results obtained by conventional PNG law for a gimbal seeker with a large FOV. (a) represents the position trajectories of a missile and a target and (b) shows a look angle of the missile. In the course of the guidance time, the look angle of the missile exceeds the FOV limit of the strapdown seeker.

(a)   (b)
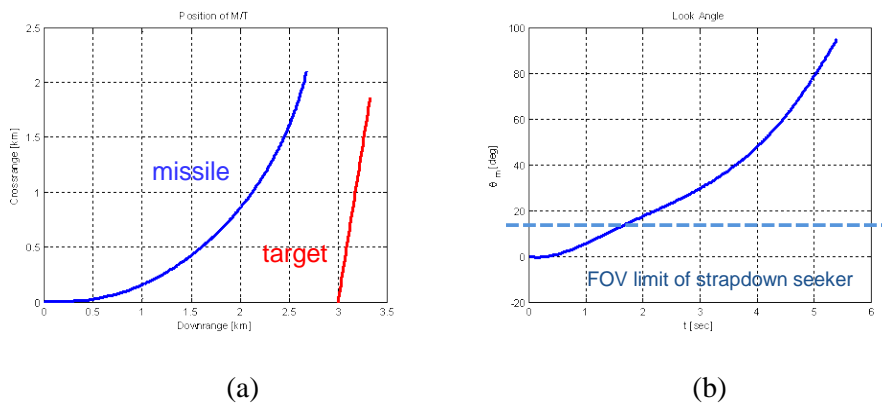
Figure 3.2: Simulation results obtained by conventional PNG law for a strapdown seeker with a narrow FOV. (a) represents the position trajectories of a missile and a target and (b) shows a look angle of the missile. The target is outside of the missile's view after about 1.5 [sec].

has no FOV constraint; in other words, the missile uses the gimbal seeker.

The PNG shows good performance for the missile installing the gimbal seeker against targets moving at a constant velocity, as shown in Fig 3.1(a). However, the look angle increases by about 25 [deg] over the course of the guidance time as depicted in Fig 3.1(b). Considering the strapdown seeker, the FOV limit of the strapdown seeker is a maximum of ±15 [deg]. In this case, the look angle over the course of the guidance by the PNG law moves to beyond the FOV limit of the strapdown seeker. Fig 3.2 presents the guidance performance when the strapdown seeker is attached to the missile. As shown in Fig 3.2(a), the missile fails the tactical mission to intercept the target. The mission fails because the look angle of the missile deviates from the limit of the strapdown seeker at about 1.5 [sec].

In order to solve the problem mentioned above, we propose a hybrid guidance (HG) law. We assume the following for simplicity of derivation of the HG law.

A1) The antenna centerline is aligned with the missile centerline.

A2) Seeker dynamics are fast enough to be neglected.

A3) The missile and the target are considered as geometric points moving in the pitch plane.

A4) The missile angle-of-attack is ignored.

A5) The missile velocity V_m and target velocity V_t are constant.

A6) The autopilot has first order dynamics.

Assumptions A1 and A2 are associated with the strapdown seeker. Because the strapdown seeker is rigidly mounted on the missile, the antenna centerline of the seeker coincides with that of the missile body. Moreover, in order to focus on the dynamics of the autopilot according to A6, the seeker dynamics are neglected. Also, A3~A5 are related to the engagement geometry. The general three-dimensional guidance can be dealt with by resolving an applied acceleration of missile into two lateral planes by neglecting the cross-coupling between the two orthogonal components such as pitch and yaw plane. We consider only the two-dimensional planar guidance for deriving the HG law. Since the HG law uses the pure proportional navigation guidance (PPNG) law, the engagement geometry of the missile and the target can be depicted as shown in Fig 3.3.

The target moves with the velocity V_t and the lateral acceleration a_t. The missile chases the target with the velocity V_m and the lateral acceleration a_m. The lateral acceleration a_m is obtained by an acceleration command a_{mc} through the first order dynamics with time constant τ. The strapdown seeker measures the look angle θ_m which depends on the attitude of the missile and the LOS angle σ. The LOS angle σ which is used in PNG law is obtained by combining the look angle and the attitude of
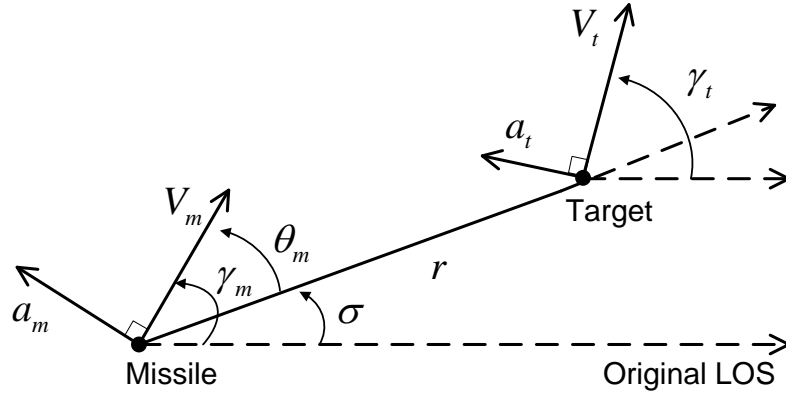
Figure 3.3: Engagement geometry of the proposed HG law.

the missile. From A3 and A5, the missile flight path angle γ_m replaces the attitude of the missile.

Based on the engagement geometry of Fig 3.3, the kinematics and dynamics are obtained as follows.

$$\dot{\gamma}_t = \frac{a_t}{V_t}, \tag{3.1}$$

$$\dot{\gamma}_m = \frac{a_m}{V_m}, \tag{3.2}$$

$$\dot{r} = V_t \cos\theta_t - V_m \cos\theta_m, \tag{3.3}$$

$$r\dot{\sigma} = V_t \sin\theta_t - V_m \sin\theta_m, \tag{3.4}$$

where θ_t, θ_m, and a_{mc} are defined by

$$\theta_t = \gamma_t - \sigma, \tag{3.5}$$

$$\theta_m = \gamma_m - \sigma, \tag{3.6}$$

$$a_m = \frac{1}{\tau s + 1} a_{mc}, \tag{3.7}$$

where τ and γ_t are the time constant and target flight angle, respectively.

3.1.2 The Overall Scheme

The PNG law is the most widely used in the guidance because it is easily implemented and has a good homing guidance performance. However, the missile often fails to chase the high speed target when the strapdown seeker is used. We propose an alternative, the hybrid guidance (HG) law, which combines two guidance laws of the proportional navigation guidance (PNG) law and the sliding mode guidance (SMG) law. The two guidance laws switch positions at a particular look angle θ_m; this is called the switching boundary $\theta_m(t_{switch})$. Fig 3.4 describes the concept of the HG law. In the first phase, ⓐ, where the look angle is within the switching boundary, the PNG law controls the missile. In the second phase, ⓑ, on the other hand, where the look angle is over the switching boundary, the SMG law is adopted to ensure the look angle remains within the FOV limit. The aim of selecting the switching boundary is to use the PNG law as much as possible during the overall homing phase and to ensure

the look angle remains within the limit of the FOV. Fig 3.5 shows the entire scheme of hybrid guidance law. While the missile is guided by the PNG law in the first phase, a

(a)   (b)
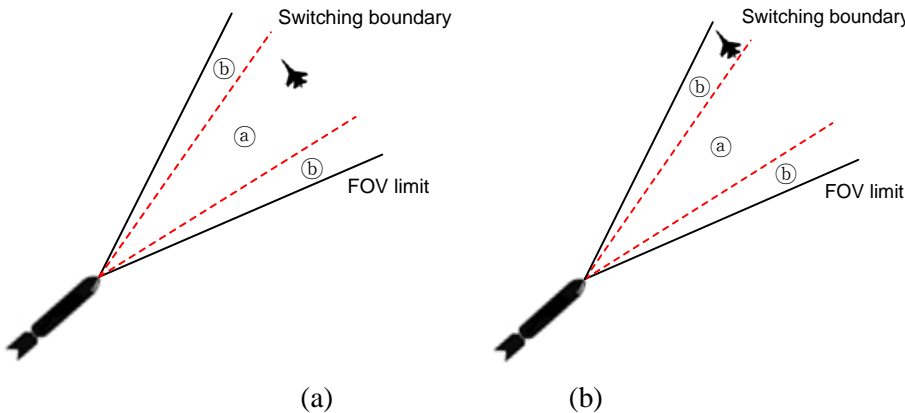
Figure 3.4: Engagement cases divided into two phases – (a) the first phase and (b) the second phase. A switching boundary differentiates the first phase and the second phase. In the first phase, PNG law is applied, while in the second phase, the SMG law is adopted.
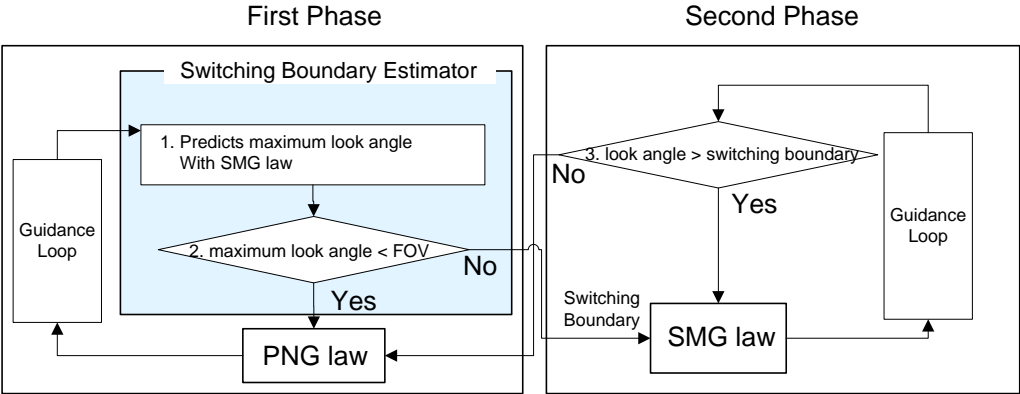
Figure 3.5: Scheme of Hybrid guidance law.

maximum look angle is estimated on-line by simulating the virtual guidance scenario using the SMG law based on the current look angle. When the estimated maximum look angle reaches the FOV limit, the second phase is started and the current look angle is regarded as the switching boundary. In the second phase, SMG law controls the missile while the look angle is larger than the switching boundary. When the look angle is less than the switching boundary, the first phase is adopted again. This logic is iterated until the missile intercepts the target.

3.1.3 Guidance Law for the First Phase

Recently, a proportional navigation guidance (PNG) law has been widely used for tactical application. The PNG law can be derived to null the LOS rate. Among various PNG laws, we use the pure PNG (PPNG) law which generates the acceleration command perpendicular to the velocity vector for the missile.

$$a_{mc} = N_1 V_m \dot{\sigma}, \tag{3.8}$$

where N_1 is a unitless designer chosen gain which is usually within the range of 3~5. In this chapter, we use an N_1 of 3.

3.1.4 Guidance Law for the Second Phase

The sliding mode control methodology is used in the derivation of the second phase

guidance law. In order to apply the sliding mode control, we set a switching surface. The guidance goal in this phase is to reduce the look angle against the high speed target. Hence, the switching surface should be chosen such that

$$S(t) = \theta_m(t). \tag{3.9}$$

The basic goal for the selection of the above switching surface is to decrease the look angle. The next step involves designing a control law that satisfies the sliding condition. To achieve this, we consider the time derivative of a Lyapunov function $V = S^2(t)/2$

$$
\begin{aligned}
\dot{V} &= S(t)\dot{S}(t) \\
&= \theta_m(t)\dot{\theta}_m(t) \\
&= \theta_m(t)\left(\dot{\gamma}_m(t) - \dot{\sigma}(t)\right) \\
&= \theta_m(t)\left(\frac{a_m(t)}{V_m} - \dot{\sigma}(t)\right).
\end{aligned}
\tag{3.10}
$$

It is assumed that the autopilot dynamics are ignored, i.e. $a_m(t) = a_{mc}(t)$. A choice for the control $a_{mc}(t)$ which will ensure that the derivative of the Lyapunov function is less than zero is

$$a_{mc}(t) = V_m\dot{\sigma}(t) - N_2\,\mathrm{sgn}(\theta_m), \tag{3.11}$$
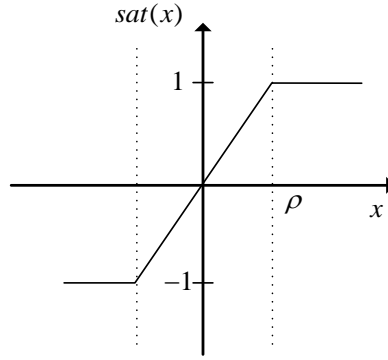
Figure 3.6: Saturation function.

where $N_2 > 0$ is constant. Also, $\mathrm{sgn}(\theta_m)$ is a sign function as

$$\mathrm{sgn}(x) = \begin{cases} 1 & \text{if } x > 0 \\ 0 & \text{if } x = 0 \\ -1 & \text{if } x < 0 \end{cases}. \tag{3.12}$$

Here, the sign function $\mathrm{sgn}(\cdot)$ causes a chattering phenomenon in practice due to the discontinuity in the vicinity of the switching surface. A solution to cope with chattering is the use of a saturation function $\mathrm{sat}(\cdot)$, instead of $\mathrm{sgn}(\cdot)$, as shown in Fig 3.6. The first term of the SMG law of Eq. (3.11) is an acceleration value to ensure the look angle remains steady. The second term influences the degree to guide the look angle to zero.

3.1.5 Switching Boundary Estimation

If the missile is guided only by the SMG law, it is steered so that the velocity vector

of the missile points at the target at each instant in time. Then, as the missile approaches closer to the target, it requires greater lateral acceleration command to be able to turn towards the target. Finally, the lateral acceleration command exceeds the missile hardware limit and the missile fails to intercept the high speed target. On the other hand, this problem does not arise with the PNG law as it orients the missile to an estimated interception point. This difference means that the PNG law has better intercept performance against the high speed target than the SMG law. Therefore, it is important to determine the switching boundary $\theta_m(t_{switch})$ to use the PNG law as much as possible during the overall homing phase.

Meanwhile, because some delays occur between $a_m(t)$ and $a_{mc}(t)$ in an actual situation, the look angle is increased gradually for a certain time, even though the SMG law is adopted. The pattern of the look angle in the second phase is influenced by the characteristic of the guidance system (such as system delay) and the engagement (such as missile velocity and look angle rate) etc. In order for the patterns of the look angle in the second phase to be as similar to each other as possible in spite of various engagements, the gain N_2 is determined by

$$N_2 = \rho \tau V_m \, | \dot{\theta}_m(t_{switch}) |, \tag{4.13}$$

where τ, V_m, $\rho > 0$, and t_{switch} are the time constant, missile velocity, the

proportional gain, and the switching time from the first phase to the second phase,
respectively. Also, $|\dot{\theta}_m(t_{switch})|$ is an absolute value of a look angle rate at the time
t_{switch}.

As shown in Fig 3.7, assume that the guidance law is changed from the first phase to
the second phase at a time t. When the look angle reaches its peak at the time $t+\hat{T}_t$, the
maximum values of the look angle and $\hat{T}_t$ are estimated by using parameters of time t.
To estimate the above values, we assume the following.

$$\hat{\dot{\sigma}}(s) = \dot{\sigma}(t), \ s \in [t, t+\hat{T}_t].   \tag{3.14}$$

where $\hat{\dot{\sigma}}(\cdot)$ is an estimated value of the LOS angular rate. Then, the estimated
acceleration command is

$$\begin{aligned}\hat{a}_{mc}(s) &= V_m \hat{\dot{\sigma}}(s) - \rho \tau V_m |\dot{\theta}_m(t)| \operatorname{sgn}(\theta_m(s)) \\ &= V_m \dot{\sigma}(t) - \rho \tau V_m |\dot{\theta}_m(t)| \operatorname{sgn}(\theta_m(s))\end{aligned}, \ s \in [t, t+\hat{T}_t].   \tag{3.15}$$

In the second phase, the absolute value of the look angle is sufficiently larger than
zero. Thus, we can assume that the sign of the look angle does not change during the
second phase. The estimated acceleration command can then be regarded as a constant,
as $\hat{a}_{mc}(s) = a_{mc}(t), \ s \in [t, t+\hat{T}_t]$. If the estimated acceleration command is a constant,
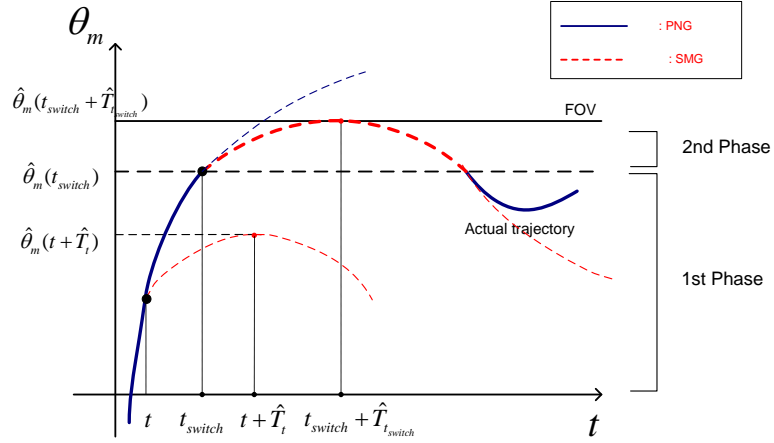
Figure 3.7: Concept of switching boundary estimation.

the estimate of the lateral acceleration is related to the estimated acceleration command.

$$\hat{a}_m(s) = e^{-(s-t)/\tau} a_m(t) + \left(1 - e^{-(s-t)/\tau}\right) a_{mc}(t), \ s \in [t, t+\hat{T}_t]. \tag{3.16}$$

Differentiating Eq. (3.6) and using Eqs. (3.2), (3.15), and (3.16), we can derive the following equation for the estimation of the look angle rate.

$$\dot{\hat{\theta}}_m(s) = \dot{\hat{\gamma}}_m(s) - \dot{\hat{\sigma}}(s)$$

$$= \frac{\hat{a}_m(s)}{V_m} - \dot{\sigma}(t)$$

$$= \frac{1}{V_m}\left\{e^{-(s-t)/\tau} a_m(t) + \left(1 - e^{-(s-t)/\tau}\right) a_{mc}(t)\right\} - \dot{\sigma}(t)$$

$$= \frac{1}{V_m}\left\{e^{-(s-t)/\tau} a_m(t) + \left(1 - e^{-(s-t)/\tau}\right)\left(V_m \dot{\sigma}(t) - \rho\tau V_m \,|\,\dot{\theta}_m(t)\,|\right) sign(\theta_m(s))\right\} - \dot{\sigma}(t)$$

$$= e^{-(s-t)/\tau} \left(\frac{a_m(t)}{V_m} - \dot{\sigma}(t) \right) - \left(1 - e^{-(s-t)/\tau} \right) \rho\tau \, | \dot{\theta}_m(t) | \, sign(\theta_m(s))$$

$$= e^{-(s-t)/\tau} \dot{\theta}_m(t) - \left(1 - e^{-(s-t)/\tau} \right) \rho\tau \, | \dot{\theta}_m(t) | \, sign(\theta_m(s)), \qquad s \in [t, t+\hat{T}_t].$$

(3.17)

We only need to consider the cases of ($\theta_m(s) \geq 0$, $\dot{\theta}_m(t) \geq 0$), and ($\theta_m(s) < 0$,

$\dot{\theta}_m(t) < 0$). Therefore,

$$\hat{\dot{\theta}}_m(s) = \dot{\theta}_m(t) \left\{ e^{-(s-t)/\tau} - \rho\tau \left(1 - e^{-(s-t)/\tau} \right) \right\}, \; s \in [t, t+\hat{T}_t]. \tag{3.18}$$

When the estimated look angle rate is zero, it reaches its peak.

$$\hat{\dot{\theta}}_m(t+\hat{T}_t) = 0, \tag{3.19}$$

where $\hat{T}_t$ satisfying (3.19) is the estimated time that elapses from the start time of the

second phase up to the time when the estimated look angle is maximum.

$$\hat{T} = -\tau \ln \left(\frac{\rho\tau}{1+\rho\tau} \right). \tag{3.20}$$

Therefore, the varied quantity of the estimated look angle during t and $t + \hat{T}_t$ is

$$\int_t^{t+\hat{T}_t} \hat{\dot{\theta}}_m(s)ds = \int_t^{t+\hat{T}_t} \left\{ e^{-(s-t)/\tau} \left(1 + \rho\tau \right) - \rho\tau \right\} \dot{\theta}_m(t)ds$$

$$= \left\{ \tau \left(1 + \rho\tau \right) \left(1 - e^{-\hat{T}_t/\tau} \right) - \rho\tau\hat{T}_t \right\} \dot{\theta}_m(t). \tag{3.21}$$

The maximum look angle which is estimated at the time t is obtained by

$$
\begin{aligned}
\hat{\theta}_{m,\max}(t) &= \theta_m(t) + \int_t^{t+\hat{T}_t} \hat{\dot{\theta}}_m(s)\,ds \\
&= \theta_m(t) + \left\{ \tau\left(1+\rho\tau\right)\left(1-e^{-\hat{T}_t/\tau}\right) - \rho\tau\hat{T}_t \right\}\dot{\theta}_m(t).
\end{aligned}
\tag{3.22}
$$

As depicted in Fig 3.7, $\hat{\theta}_{m,\max}(t)$ is smaller than the FOV of the strapdown seeker. Thus, the missile chases the target using the PNG law. We iterate this process until the updated maximum of the estimated look angle equals the FOV of the strapdown seeker. When t_{switch} is the time satisfying Eq. (3.23), the phase switches from the first phase to the second phase.

$$
\hat{\theta}_{m,\max}(t) = FOV,
\tag{3.23}
$$

where FOV is the FOV limit of the strapdown seeker. $\theta_m(t_{switch})$ is determined as the switching boundary. Also, the missile is guided by the second guidance law from this time t_{switch} until $\theta_m(t)$ is smaller than the switching boundary.

A number of errors occur between the two peaks of the actual and estimated look angles because the estimated LOS angle rate has some errors. The problem occurs in the case where the actual look angle exceeds the FOV of the strapdown seeker. The seeker lock-on condition is then broken. The missile maintains the acceleration

command at the time when it misses the target. The errors between the two peaks of the actual and estimated look angle are small and the acceleration command is large enough to decrease the look angle. Thus, even if this situation occurs, the actual look angle rapidly enters the FOV of the strapdown seeker.

3.2   Lock-on Guidance Law

This chapter proposes another new guidance law, which considers the FOV of the seeker when the missile mounts the strapdown seeker instead of the gimbal seeker. The FOV of the seeker is important for the guidance performance such as the miss distance when the strapdown seeker, which has a narrow FOV, is used in the tracking target. Moreover, because a trade-off exists between the FOV and the resolution, some cases occur whereby the seeker is implemented with narrower FOV (e.g. ± 5 [deg]) for more accurate target tracking. In these cases, the conventional guidance laws have less effective guidance performance. Research is needed to successfully complete the guidance mission with the narrower FOV of the strapdown seeker. In this chapter, we propose a new guidance law which enables the missile to chase the target despite the narrower FOV.

The proposed guidance law is called the lock-on guidance (LOG) law, which is modified from the pursuit guidance (PG) law. In the PG law, the missile is steered so that the velocity vector of the missile always points towards the target; that is, it always

has the direction of the line of sight. The concept of the PG law causes a fatal problem

of guidance performance. The missile guided by the PG law needs to take a sharp turn

near the target. Because it has a limit of maneuver, the missile cannot cover the missile

acceleration command. This would have been exaggerated if the missile had a narrow

FOV. In the case of the strapdown seeker, the missile would clearly miss the target.

3.2.1 Problem Statement

In chapter 3, we described the guidance performance of the HG law with the FOV of

the strapdown seeker by ± 15 [deg]. However, in some cases, the strapdown seeker

demands a more accurate performance of the target tracking. Assuming that the

hardware of the strapdown seeker is not changed, the accuracy of the strapdown seeker

is related to the size of the FOV. In order to explain this relation, we first introduce the

notion of an instantaneous FOV (IFOV). The IFOV, which is a measure of the spatial

resolution of a remote sensing imaging system, is defined as a solid angle subtended by

a single pixel on the axis of the imaging system. The IFOV is presented in Fig 3.8. This

element determines the spatial resolution. The IFOV is inversely proportional to the

resolution or the accuracy. The relation between the IFOV and FOV is

$$IFOV = \frac{FOV}{number\ of\ pixel}. \qquad (3.24)$$

If the number of pixels is fixed, then the IFOV is proportional to the FOV. We can
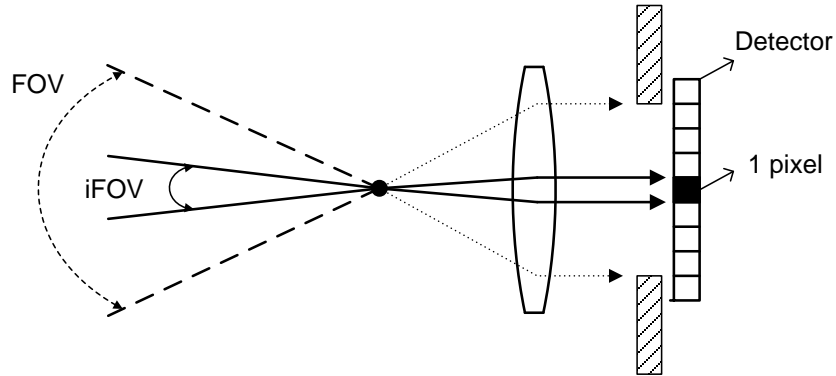
Figure 3.8: FOV and IFOV

therefore determine that the resolution is inversely proportional to the FOV. That is, the

seeker with a relatively wider FOV has a loss of angular resolution.

The measurement capability of seekers is restricted due to a number of physical,

optical, and electronic limitations such as the pixel number of the detector. In order to

increase the accuracy of the seeker, we may need to reduce the FOV of the seeker as

explained above. In this dissertation, we set the FOV by ±5 [deg]. If the FOV of the

strapdown

Table 3.1: Engagement parameters and various geometries for evaluation of HG Law
against a strapdown seeker with a narrow FOV ±5 [deg].

	Missile	Target
FOV	±5 [deg]	-
Initial velocity	680 [m/s]	350 [m/s]
Initial relative position	(0,0) [m]	(3000,0) [m]
Initial orientation	-4:1:4 [deg]	0:1:90 [deg]
Lateral acceleration limit	50g	-
Time constant	0.5 (sec)	-
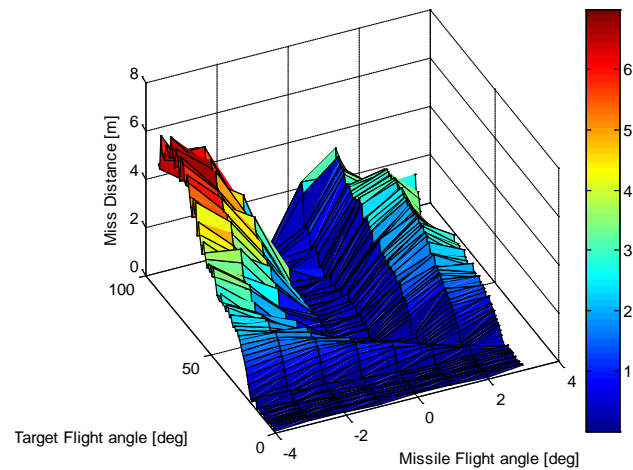
Figure 3.9: Miss distance of HG law for a strapdown seeker with a narrow FOV (± 5 [deg]) in the case of the initial flight angle of a missile by -4~4 [deg].

seeker is narrower, the performance of the conventional guidance law is less effective. The HG law also gives less effective intercept performance in the conditions shown in Table 3.1, as shown in Fig 3.9.

In order to solve the problem mentioned above, we propose another guidance law called the lock-on guidance (LOG) law. We assume the following for simplicity of derivation of the LOG law.

A1) The antenna centerline is aligned with the missile centerline.

A2) The seeker and autopilot dynamics are fast enough to be neglected.

A3) The missile and the target are considered as geometric points moving in the pitch plane.

A4) The missile angle-of-attack is ignored.

A5) The missile velocity V_m and target velocity V_t are constant.

Assumptions A1 and A2 relate to the strapdown seeker. Because the strapdown seeker is rigidly mounted on the missile, the antenna centerline of the seeker coincides with that of the missile body. Assumptions A3~A5 are related to the engagement geometry. The general three-dimensional guidance can be dealt with by resolving an applied lateral acceleration of the missile into two lateral planes, such as pitch and yaw plane, by neglecting the cross-coupling between the two orthogonal components. We consider only the two-dimensional pitch planar guidance for deriving the LOG law. The engagement geometry of the missile and the target for the LOG law can be depicted as shown in Fig 3.10. The target moves with the velocity V_t and the lateral acceleration a_t. The missile chases the target with the velocity V_m and the lateral acceleration a_m. The lateral acceleration a_m is obtained by an acceleration command without dynamics. The strapdown seeker measures the look angle θ_m which depends on an attitude of the missile and a LOS angle σ. The LOS angle σ, which is used in PG law is obtained by combining the look angle and the attitude of the missile. From A3 and A5, the missile flight path angle γ_m replaces the attitude of the missile.

Based on the above engagement geometry, the kinematics and dynamics are
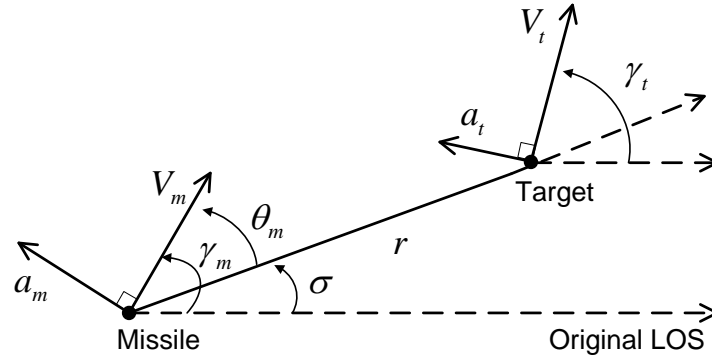
Figure 3.10: Engagement geometry of the proposed LOG law

obtained as follows.

$$\dot{\gamma}_t = \frac{a_t}{V_t}, \tag{3.25}$$

$$\dot{\gamma}_m = \frac{a_m}{V_m}, \tag{3.26}$$

$$\dot{r} = V_t \cos\theta_t - V_m \cos\theta_m, \tag{3.27}$$

$$r\dot{\sigma} = V_t \sin\theta_t - V_m \sin\theta_m, \tag{3.28}$$

where θ_t, θ_m, and a_{mc} are defined by

$$\theta_t = \gamma_t - \sigma, \tag{3.29}$$

$$\theta_m = \gamma_m - \sigma, \tag{3.30}$$

where γ_t is a target flight angle.

3.2.2 The Overall Scheme

The proposed guidance law, called the lock-on guidance (LOG) law, is based on the concept of the pursuit guidance (PG) law. However, some problems arise in the PG law. We analyze the weak points of the PG law and propose the LOG law, which compensates for the weak points of the PG law.

In the PG law, the missile is steered so that the velocity vector of the missile always points at the target; that is, it always has the direction of the line of sight. The concept of the PG law causes a fatal problem of guidance performance. The missile guided by PG law needs to take a sharp turn near the target. Because it has a limit of maneuver, the missile cannot cover the missile acceleration command. This would have been exaggerated if the missile had the narrow FOV. In the case of the strapdown seeker, the missile clearly misses the target. In this chapter, we deal with the detail of the problem of PG law. Fig 3.11 represents the trajectory of the missile guided by PG law. M0, M1, M2, and M3 are points which the missile passes and T0, T1, T2, and T3 are points which the target passes. The missile points towards the target at each instant in time. When it is located at point M3, the missile must take a very sharp turn to follow the target. However, the missile cannot take a sharp turn because the acceleration command exceeds the maneuvering capability of the missile. The solid line after point M3 is the ideal trajectory at which the missile would have followed, and eventually hit, the target, had it been capable of taking sharp turns. The broken line shows the actual
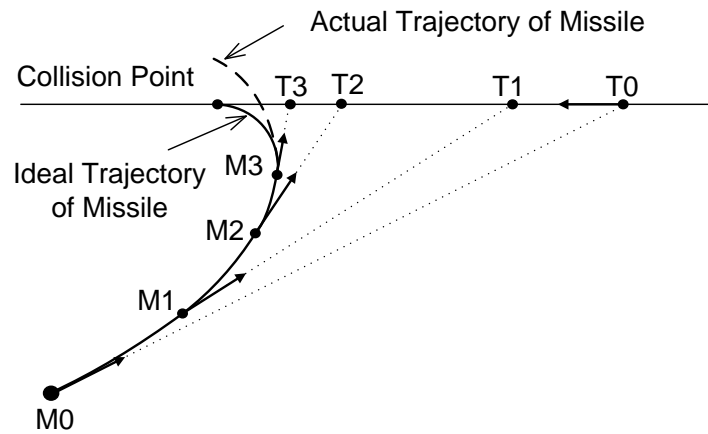
Figure 3.11: Position trajectory of a missile guided by PG law

trajectory of the missile when it is constrained by the maneuvering capability of the missile. The difference between the ideal and actual trajectory means that the missile missed the target. The LOG law solves the above cited problem of PG law in which the missile needs to be directed to take a drastic turn near the target.

The main concept of LOG law is that the FOV's edge of the strapdown seeker stares at the target rather than the center of the strapdown seeker. Designed on the basis of this concept, the missile reduces the effort required to take a sharp turn near the target because it moves before the location at which the target will later pass by. Fig 3.12 presents the concept of lock-on guidance law. M0, M1, M2, and M3 are points which the missile passes and T0, T1, T2, and T3 are points which the target passes. The FOV edge of the strapdown seeker points towards the target at each instant in time. When it is located at point M3, in the PG law case, the missile must take a very sharp
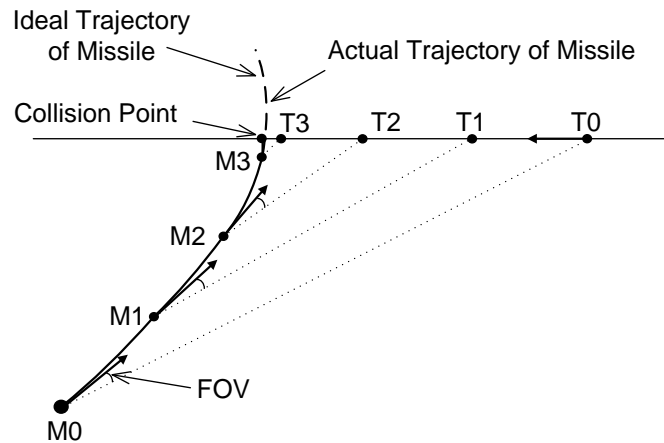
Figure 3.12: Position trajectory of a missile guided by LOG law

turn to follow the target. In the case of the LOG law, however, it is not necessity for the missile to take a sharp turn because it is moving toward the point which the target will later reach. The solid line after point M3 refers to the ideal trajectory of which the missile would have followed and eventually hit the target. The broken line shows the actual trajectory of the missile when it is constrained by the maneuvering capability of the missile. The actual trajectory can therefore almost match the ideal trajectory.

3.2.3 Derivation

In this section, we focus on the derivation of the lock-on guidance (LOG) law. To derive the LOG law, we employ the sliding mode control (SMC) methodology. SMC systems based on variable structure control (VSC) theory developed by Utkin, are distinguished by their robustness properties against a class of bounded disturbances.

Traditionally, SMC theory has found widespread usage in such diverse areas as the control of robots, aircraft, and large space structures, etc. SMC has also been applied recently in the specific field of missile guidance.

In general, the VSC system design can be broken into two phases. The first phase entails the construction of a switching surface so that the system restricted to this surface produces the desired behavior. In the next step, a control is selected that will drive the system trajectories onto the switching surface and constrain them to slide along this surface for all subsequent times. Since the desired surface is chosen such that it is independent of the external disturbances, robustness can be achieved.

To design the guidance law according to VSC theory, a switching surface that represents the desired system dynamics needs to be selected. The selection of the switching surface is crucial because the structure of the guidance law and its robustness properties are considerably dependent on it.

We have demonstrated that PNG law is unsuitable for the missile with the strapdown seeker. We therefore design the LOG law by modifying the concept of the PG law. In the PG law concept, the switching surface is set by $S = \theta$. This switching surface means that the missile stares directly at the target. However, in the LOG law concept, the switching surface is set so that the FOV edge of the strapdown seeker mounted the missile stares at the target. The switching surface is

$$S = sign(\theta_t) \cdot (FOV - \varepsilon) - \theta_m, \quad \varepsilon > 0. \tag{3.31}$$

The basic aim of the selection of the above switching surface is to square the look

angle θ_m with the FOV edge. Fig 3.13 makes the above selection of the switching

surface easier to understand. In order to locate the target on the line of the FOV edge of

the missile seeker, we need to consider two cases. As shown in Fig 3.13(a), when the

flight path angle of the target is more than zero $\theta_t > 0$, the acceleration command

needs to be generated such that the look angle θ_m corresponds to the FOV edge A,

which is expressed by the angle of $FOV - \varepsilon$. Similarly, when the flight path angle of

the target is less than zero $\theta_t < 0$ as shown in Fig 3.13(b), the acceleration command

needs to be generated such that look angle θ_m corresponds to the FOV edge B, of

which the angle is $-(FOV - \varepsilon)$. Eq. (3.31) is the switching surface for satisfying the

above physical geometry requirement. Assume that we can achieve

$sign(\theta_t) \cdot (FOV - \varepsilon) - \theta_m = 0$ by a suitable choice of control. The missile can then

track the target for all guidance times. Because the velocity of the missile is greater

than the target, according to assumption A5 which implies that $\dot{R} < 0$, interception is

guaranteed.

The next step involves designing a control law that will guarantee the attractivity of

the surface $S = 0$ as well as the sliding ability $S = 0$. To achieve this, we construct

the

following Lyapunov function:
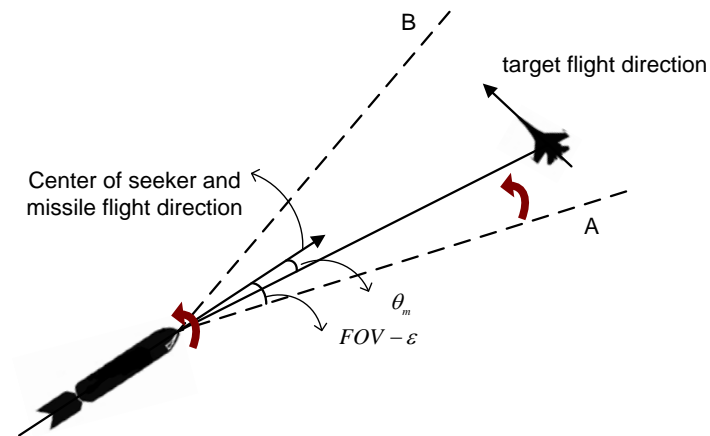
(a)
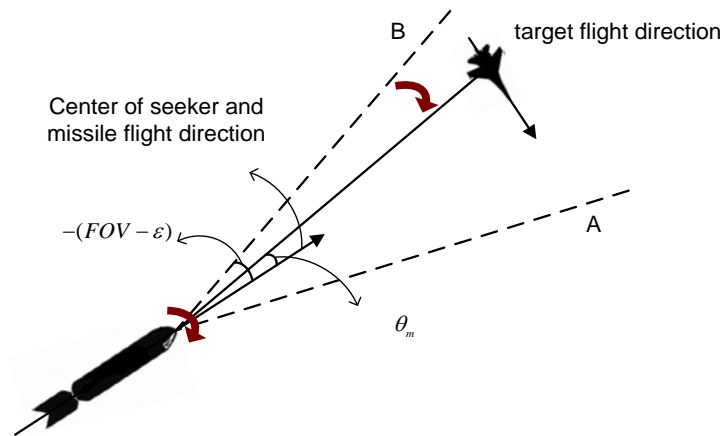
(b)

Figure 3.13: Engagement cases of (a) $\theta_t > 0$ and (b) $\theta_t > 0$ for selecting switching surface. In the case of (a) and (b), the switching surfaces are $S = (FOV - \varepsilon) - \theta_m$ and $S = -(FOV - \varepsilon) - \theta_m$, respectively. Synthetically, the switching surface is $S = sign(\theta_t) \cdot (FOV - \varepsilon) - \theta_m,\ \varepsilon > 0.$

$$V = \frac{1}{2}S^2.$$

(3.32)

To guarantee the attractivity of $S = 0$ is used to ensure

$$\dot{V} = \dot{S}S < 0, \quad \text{for } S \neq 0.$$

(3.33)

Substituting Eq. (3.31) into Eq. (3.33), the time derivative of a Lyapunov function with $\dot{\theta}_m > 0$ is

$$\begin{aligned}
\dot{V} &= S\dot{S} \\
&= (FOV - \varepsilon - \theta_m)(-\dot{\theta}_m) \\
&= (FOV - \varepsilon - \theta_m)(-\frac{a_m}{V_m} + \dot{\sigma}).
\end{aligned}$$

(3.34)

A choice of the acceleration command a_{mc} that ensures $\dot{V} < 0$ under A6 is

$$\begin{aligned}
a_{mc} &= V_m\dot{\sigma} + V_m(FOV - \varepsilon - \theta_m) \\
&= V_m\dot{\sigma} - V_m\theta_m + V_m(FOV - \varepsilon).
\end{aligned}$$

(3.35)

Similarly, the time derivative of a Lyapunov function with $\dot{\theta}_m < 0$ is

$$\begin{aligned}
\dot{V} &= S\dot{S} \\
&= (-FOV + \varepsilon - \theta_m)(-\dot{\theta}_m) \\
&= (FOV - \varepsilon + \theta_m)(\frac{a_m}{V_m} - \dot{\sigma}).
\end{aligned}$$

(3.36)

A choice of the acceleration command a_{mc} that ensures $\dot{V} < 0$ under A6 is

$$
\begin{aligned}
a_{mc} &= V_m \dot{\sigma} - V_m (FOV - \varepsilon + \theta_m) \\
&= V_m \dot{\sigma} - V_m \theta_m - V_m (FOV - \varepsilon).
\end{aligned}
\tag{3.37}
$$

Synthesizing Eq. (3.35) and Eq. (3.37), the acceleration command a_{mc} is

$$
a_{mc} = V_m \dot{\sigma} - V_m \theta_m + sign(\theta_t) V_m (FOV - \varepsilon),
\tag{3.38}
$$

where

$$
\mathrm{sgn}(x) = \begin{cases} 1 & \text{if } x > 0 \\ 0 & \text{if } x = 0 \\ -1 & \text{if } x < 0 \end{cases}.
\tag{3.39}
$$

Here, the sign function $\mathrm{sgn}(\cdot)$ causes a chattering phenomenon in practice due to the discontinuity in the vicinity of the switching surface. A solution to cope with chattering is to use a saturation function $\mathrm{s}\,at(\cdot)$ instead of $\mathrm{sgn}(\cdot)$.

Chapter 4

Simulation Results

The proposed guidance laws are verified through simulation. In order to obtain meaningful performance evaluation, a number of different engagement geometries were utilized. The engagement geometries are classified overall into two groups: nonmaneuvering target and maneuvering target. Target maneuvers are always made normal to the velocity vector and with a constant acceleration (g) level. In each case, the simulation is carried out by changing the initial flight angle of a missile and target. The simulations have several common parameters: the target initially flies 3 km from the missile; the velocities of the missile and the target are 680 [m/s] and 350 [m/s], respectively; the applied lateral acceleration is limited by 50 [g]; the simulation is terminated when the closing velocity of the missile and the target is less than zero; and the separation range at the intercept time is taken as the measure of miss distance.

4.1 Hybrid Guidance Law

4.1.1 Nonmaneuvering Target

In this subchapter, verification of the proposed hybrid guidance (HG) law is conducted through simulation. The engagement geometry and conditions of the simulation for evaluation of HG law are presented in Table 4.1. It is assumed that the

autopilot has first order dynamics with a time constant of 0.5 [s] and that the limit of the FOV of the strapdown seeker is ±15 [deg]. The simulation results are presented in Fig 4.1. For the purpose of comparison, the conventional PNG law is employed in this simulation. The conventional PNG law is the PPNG law. In Fig 4.1(a), the dashed line and the solid line represent the position trajectories of the missile by the PPNG law and the HG law, respectively. The dotted line indicates the target trajectory at high speed. The missile guided by the PPNG law travels beyond the FOV of the strapdown seeker after 2 [s] and fails to intercept the target. The reason for this simulation result is that the look angle of the missile lying on the collision course is required to be a higher value than the limit of the FOV. The look angle deviates from the limit of the FOV while attempting to align with the collision course. On the other hand, the missile guided by the proposed HG law maintains the seeker lock-on condition until it approaches close to the target. Whenever there is a possibility that the look angle will be larger than the limit of the FOV, the second phase guidance law reduces the look angle. Comparing the two guidance laws in terms of performance criteria of miss distance, the miss distances of the PPNG law and the HG law are about 716 [m] and 0.66 [m], respectively.

The various engagements are tabulated in Table 4.2. The initial missile flight angle is increased by 1 [deg] from -14 to 14 [deg] and the initial target flight angle is increased by 1 [deg] from 0 to 90 [deg]. The capturability of a guidance law is defined as its

ability to ensure capture or interception of a target by a missile. This is an important

concept in the performance evaluation of missile guidance laws. The capture region is

defined as the collection of all initial conditions from which a missile can intercept a

target, and is a measure of the capturability performance of the guidance law. The

capture region is presented in Fig 4.2. The white areas show that the miss distance of

the missile and the target is within 2 [m]; that is, the missile captured the target. The

black areas show that the miss distance of the missile and target is over 2 [m]. Fig 4.2(a)

shows that the missile guided by the PNG law is able to chase the flying target at a low

flight path angle. However, when the target lies at a flight path angle of above about 40

[deg], the missile guided by the PNG law cannot chase the target. The capturability

performance of the HG law is superior to that of the PNG law as shown in Fig 4.2(b).

The miss distances for several cases of engagements are depicted in Fig 4.3. When the

target has an initial flight angle smaller than 40 [deg], the miss distances of the two

guidance laws are same because the look angle does not deviate from the FOV limit,

even when using only the PNG law. When the initial flight angle of the target is larger

than 40 [deg], the HG law can chase the target by iterating the switch of the first phase

and second phase during the course of guidance. However, when the missile is

launched with an initial flight angle of less than -10 [deg], the guidance performance of

the HG law is poor because the look angle of the missile launched is larger than the

switching boundary. Except for these engagement cases, the miss distances are within 3

[m].

Table 4.1: Engagement parameters and geometry for evaluation of HG law against nonmaneuvering target at high speed

	Missile	Target
FOV	±15 [deg]	-
Initial velocity	680 [m/s]	350 [m/s]
Initial relative position	(0,0) [m]	(3000,0) [m]
Initial orientation	0 [deg]	60 [deg]
Lateral acceleration limit	50g	-
Time constant	0.5 [sec]	-

Table 4.2: Engagement parameters and various geometries for evaluation of HG law against nonmaneuvering target at high speed

	Missile	Target
FOV	±15 [deg]	-
Initial velocity	680 [m/s]	350 [m/s]
Initial relative position	(0,0) [m]	(3000,0) [m]
Initial orientation	-14:1:14 [deg]	0:1:90 [deg]
Lateral acceleration limit	50g	-
Time constant	0.5 [sec]	-

(a)

(b)

(c)

(d)
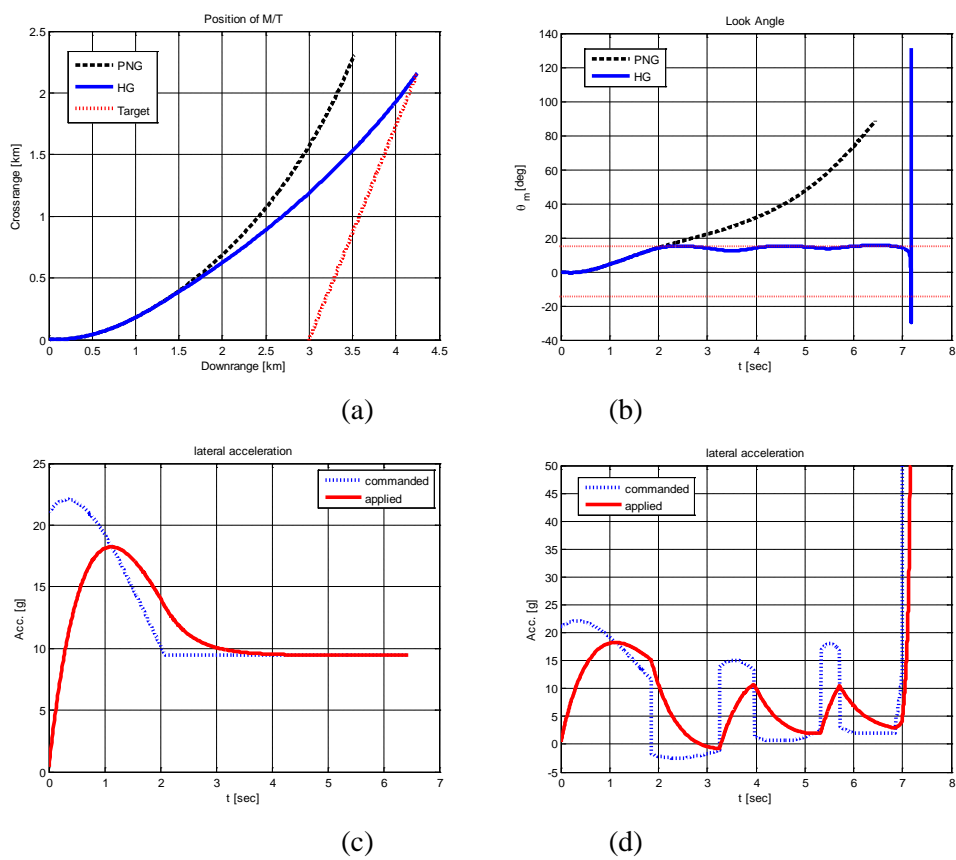
Figure 4.1: Simulation results of PNG and HG law under conditions given in Table 4.1. (a) position trajectories of missiles guided by two guidance laws and a target, (b) look angle of the missile, (c) commanded and applied lateral accelerations in the case of missile guided by PNG law, and (d) commanded and applied lateral accelerations in the case of missile guided by proposed HG law.
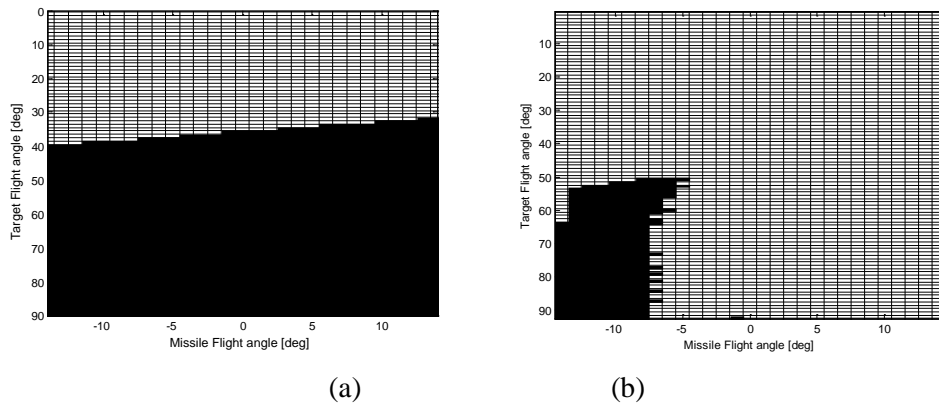
Figure 4.2: Capture region of (a) PNG and (b) HG law under conditions given in Table 4.2. The white areas show where the miss distance is within 2 [m] and the black areas show where the miss distance is over 2 [m].
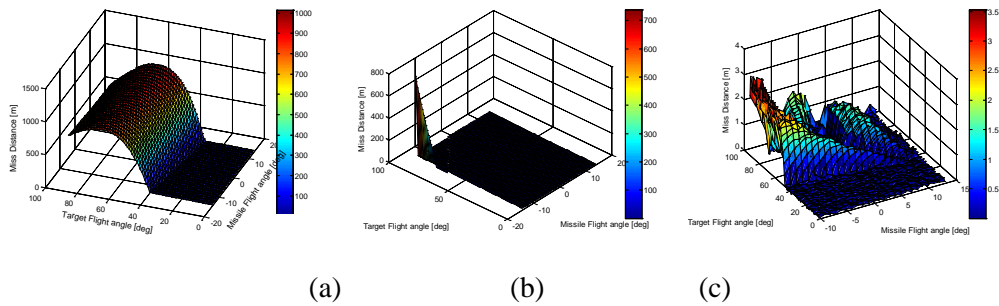
Figure 4.3: Miss distances of (a) PNG and (b, c) HG laws under conditions given in Table 4.2. (a) shows miss distance of PNG law in the case of initial flight angle of a missile at -14~14 [deg]. (b) and (c) show miss distances of HG law in the case of initial flight angle of the missile at -14~14 [deg] and -10~14 [deg], respectively.

4.1.2 **Maneuvering Target**

To evaluate the potential of the newly proposed HG law against a maneuvering target, a performance evaluation is carried out using a simulation for the low (2g) and medium (6g) maneuvering targets. We used a simulation to ensure that the strapdown seeker cannot tolerate high (8g) maneuvering target. The simulation results on the high maneuvering target are omitted in this dissertation since other simulation results are sufficient to evaluate the guidance performance of the proposed HG law against a maneuvering target.

<u>Low Maneuvering Target</u>

Table 4.3 lists the engagement parameters and geometry for evaluation of the HG law against a low maneuvering target, whereby the target initiates a $-2g$ dive turn at the beginning of interception, switches to level flight after 2 [sec], and then executes a $2g$ evasive maneuver after 1 second and continues until interception. In addition, a time constant of the first autopilot dynamics is 0.5 [sec] and the limit of the FOV of the strapdown seeker is ±15 [deg]. Fig 4.4 presents simulation results of the PNG law and the HG law under the conditions listed in Table 4.3. The missile guided by PNG law misses the target a few seconds after the target switches to level flight, and then fails to intercept the target. However, the missile guided by HG law maintains the lock-on condition until interception and successfully completes the engagement with a miss distance of 0.422 [m]. We then analyze the performance of the HG law against a low

maneuvering target for the opposite condition. Table 4.3 shows engagement parameters and geometry against a low maneuvering target and Fig 4.5 presents simulation results of the PNG law and the HG law under the condition listed in Table 4.4. Similarly, the missile guided by the PNG law misses the target at the time the target switches to level flight, and then fails interception. The missile employing the HG law then completes the engagement with a miss distance of 13.28 [m]. Thus, the guidance performance of the proposed HG law is rather unsatisfactory. This simulation result occurs because the switching boundary estimator in the proposed HG law cannot accurately estimate the switching timing from the first phase to the second phase because the target maneuvers deviate from the FOV of the missile.

Table 4.3: Engagement parameters and geometry for evaluation of HG law against low maneuvering target, $-2g\,(0 < t < 2),\ 0g\,(2 < t < 3),\ 2g\,(3 < t)$
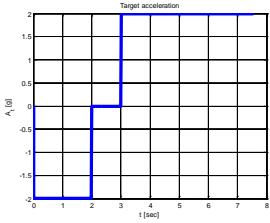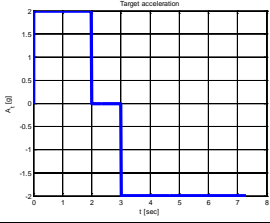
	Missile	Target
FOV	±15 [deg]	-
Initial velocity	680 [m/s]	350[m/s]
Initial relative position	(0,0) [m]	(3000,0)[m]
Initial orientation	0 [deg]	60 [deg]
Lateral acceleration limit	50g	-
Time constant	0.5 [sec]	-
Maneuver	-	

Table 4.4: Engagement parameters and geometry for evaluation of LOG law against low maneuvering target, $2g\,(0 < t < 2),\ 0g\,(2 < t < 3),\ -2g\,(3 < t)$

	Missile	Target
FOV	±15 [deg]	-
Initial velocity	680 [m/s]	350[m/s]
Initial relative position	(0,0) [m]	(3000,0)[m]
Initial orientation	0 [deg]	60 [deg]
Lateral acceleration limit	50g	-
Time constant	0.5 (sec)	-
Maneuver	-	

(a)　　　　　　　　　(b)

(c)　　　　　　(d)

Figure 4.4: Simulation results of PNG and HG law under conditions shown in Table 4.3. (a) shows position trajectories of missiles guided by several guidance laws and a target, and (b) shows look angles of the missile. (c) and (d) show commanded and applied lateral accelerations in the case of a missile guided by the PNG and proposed HG law, respectively. The missiles guided by PNG and HG laws miss at about 2 [sec], and 7.2 [sec] (which is immediately before interception), respectively. The mission adopting the PNG law fails to intercept. In the case of HG law, the miss distance is about 0.548[m].

(a)   (b)

(c)   (d)
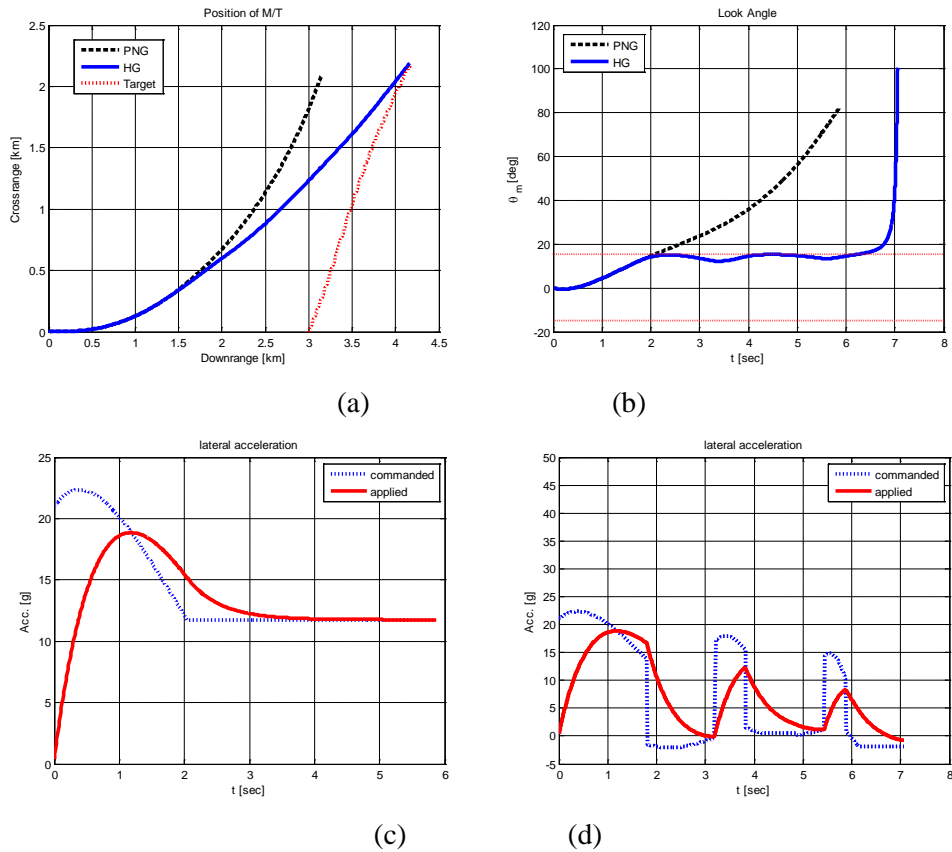
Figure 4.5: Simulation results of PNG and HG laws under conditions given in Table 4.4. (a) shows position trajectories of missiles guided by several guidance laws and a target, and (b) shows look angles of the missiles. (c) and (d) show commanded and applied lateral accelerations in the case of the missile guided by PNG and proposed HG law, respectively. The missiles guided by PNG and HG law miss at about 2 [sec] and 6 [sec], respectively. The mission adopting the PNG law fails to intercept. In the case of HG law, the miss distance is about 13.28 [m].

Medium Maneuvering Target

Table 4.5 (Table 4.6) lists the engagement parameters and geometry for evaluation of HG law against a medium maneuvering target, whereby the target initiates a $-6g$ ($6g$) dive turn at the beginning of interception, switches to level flight after 2 [sec], and then executes a $6g$ ($-6g$) evasive maneuver after 1 second and continues until interception. Fig 4.6 (Fig 4.7) represents simulation results of the PNG law and the HG law under the conditions listed in Table 4.5 (Table 4.6). An unusual result can be seen in Fig 4.6, where it appears that the guidance performance of the PNG law against the medium maneuvering target is better than that against the low maneuvering target. This is by chance. The target disappears from the view of the missile guided by the PNG law at an early stage and only a few seconds later, the target comes into view of the missile only by chance. The PNG law is thus also not appropriate for these engagements. On the other hand, under the conditions listed in Table 4.5, the missile guided by HG law maintains the lock-on condition until interception and successfully completes the engagement with a miss distance of 2.04 [m]. However, in the case of the condition in Table 4.6, the missile employing the HG law completes the engagement, with a miss distance of 79.19 [m]. Thus, such guidance performance of the proposed HG law is not satisfactory. This simulation result occurs for the same reason as that for the simulation result mentioned in the above section.

Table 4.5: Engagement parameters and geometry for evaluation of LOG law against low maneuvering target, $-6g(0 < t < 2)$, $0g(2 < t < 3)$, $6g(3 < t)$
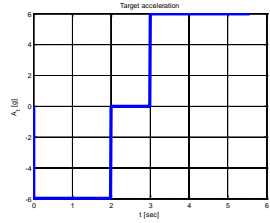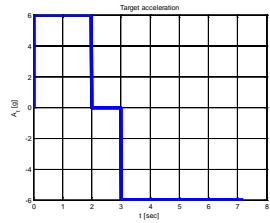
	Missile	Target
FOV	±15 [deg]	-
Initial velocity	680 [m/s]	350[m/s]
Initial relative position	(0,0) [m]	(3000,0)[m]
Initial orientation	0 [deg]	60 [deg]
Lateral acceleration limit	50g	-
Time constant	0.5 (sec)	-
Maneuver	-	

Table 4.6: Engagement parameters and geometry for evaluation of LOG law against low maneuvering target, $6g(0 < t < 2)$, $0g(2 < t < 3)$, $-6g(3 < t)$

	Missile	Target
FOV	±15 [deg]	-
Initial velocity	680 [m/s]	350[m/s]
Initial relative position	(0,0) [m]	(3000,0)[m]
Initial orientation	0 [deg]	60 [deg]
Lateral acceleration limit	50g	-
Time constant	0.5 (sec)	-
Maneuver	-	

Figure 4.6: Simulation results of PNG and HG law under conditions shown in Table 4.5. (a) shows position trajectories of missiles guided by several guidance laws and a target and (b) shows look angles of the missile. (c) and (d) show commanded and applied lateral accelerations in the case of a missile guided by the PNG and proposed HG law, respectively. The missiles guided by PNG law miss at about 2.5 [sec] and after about 3 seconds the target enters the FOV of the missile by chance for a few seconds. In the case of HG law, the miss distance is about 2.04 [m] at the time of interception.
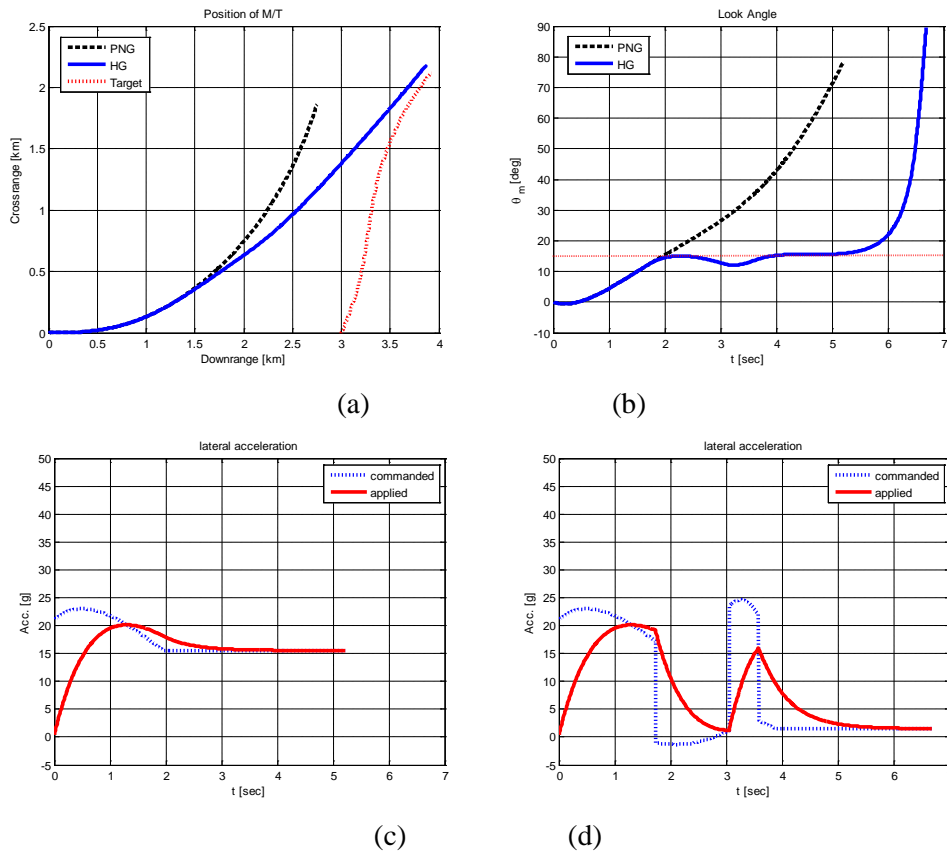
Figure 4.7: Simulation results of PNG and HG law under conditions shown in Table 4.6. (a) shows position trajectories of missiles guided by several guidance laws and a target and (b) shows the look angles of the missile. (c) and (d) show commanded and applied lateral accelerations in the case of a missile guided by the PNG and proposed HG laws, respectively. The missiles guided by the PNG and HG laws miss at about 2 [sec] and 3.5 [sec], respectively. Both guidance laws fail to intercept the target.

4.2 **Lock-on Guidance Law**

4.2.1 **Nonmaneuvering Target**

<u>**Case I: Ideal Autopilot Dynamics**</u>

In case I, all dynamics of the guidance loop are neglected. In this case, the guidance performance of a lock-on guidance (LOG) law is verified through simulation. All of the simulation data are generated in a variety of geometric scenarios.

First, in order to show the position trajectory of the missile and the target, and the look angle of the missile, we simulated using a specific engagement geometry. The FOV of the strapdown seeker is ±5 [deg]. The engagement data of the missile and the target are shown in Table 4.7, while the simulation results are presented in Fig 4.8. For the purpose of comparison, the conventional PNG law such as a pure PNG (PPNG) and PG laws are employed in this simulation. In Fig 4.8(a), the dashed line, dotted line, and the solid line represent the trajectories of the missile by the PPNG law, the PG law, and the proposed guidance law, respectively. The curved dotted line indicates the target trajectory at high speed. The missile guided by the PPNG law travels beyond the FOV of the strapdown seeker as soon as it launches and fails to intercept the target. The missile guided by PG law shows the performance of somehow intercepting the target. However, as shown in Fig 4.8(b), the look angle of the missile guided by PG law fluctuates and is very unstable near the target. On the other hand, the missile guided by the proposed LOG law maintains the seeker lock-on condition for the entire guidance

time. Comparing the performance of the miss distances, the three guidance laws of PPNG law, PG law, and LOG law are about 943.93m, 1.86m, and 0.0007m, respectively.

Fig 4.9 shows whether or not the missile maintains the lock-on condition according to using the various guidance laws. We increased the initial missile flight angle by 1deg from -4deg to 4deg and increased the initial target flight angle by 1deg from 0deg to 90deg. Other engagement data concurs with those of Table 4.7. The engagement data of the missile and the target are summarized in Table 4.3. In Fig 4.9, the white area shows where the missile maintains the lock-on condition until intercepting the target and the black area represents the failure of the lock-on condition during an intercepting task. Fig 4.9 demonstrates the outstanding performance of the LOG law compared with the PPNG law and PG law. As shown in Fig 4.9(a), the PPNG law is the least effective at maintaining the lock-on condition when the missile is equipped with the strapdown seeker. Fig 4.9(b) shows the performance of the PG law in maintaining the lock-on condition. Fig 4.9(c), the missile guided by the LOG law successfully accomplished the interception task while maintaining the lock-on condition. Fig 4.10 shows the miss distance in various engagement conditions. In Fig 4.10(a), the PNG law showed good guidance performance within the target initial flight angle by about 10 [deg] because it could ensure that the missile was guided with a lock-on condition. However, the miss distance was increased exponentially above about 10 [deg], since the missile missed

the target and strayed off course. Fig 4.10(b) shows that, except for some areas, the PG law could maintain the lock-on condition with the given engagement conditions. However, this simulation result also includes the impossible maneuver of the missile in the actual system. In the LOG law case, it is possible that the missile could intercept the target because the lock-on condition was maintained.

Table 4.7: Engagement parameters and geometry for evaluation of LOG law against nonmaneuvering target at high speed (Case I: ideal autopilot dynamics)

	Missile	Target
FOV	±5 [deg]	-
Initial velocity	680 [m/s]	350 [m/s]
Initial relative position	(0,0) [m]	(3000,0) [m]
Initial orientation	0 [deg]	90 [deg]
Lateral acceleration limit	50g	-

Table 4.8: Engagement parameters and various geometries for evaluation of LOG law against nonmaneuvering target at high speed (Case I: Ideal autopilot dynamics)

	Missile	Target
FOV	±5 [deg]	-
Initial velocity	680 [m/s]	350 [m/s]
Initial relative position	(0,0) [m]	(3000,0) [m]
Initial orientation	-4:1: 4 [deg]	0:1:90 [deg]
Lateral acceleration limit	50g	-

(a)   (b)

(c)
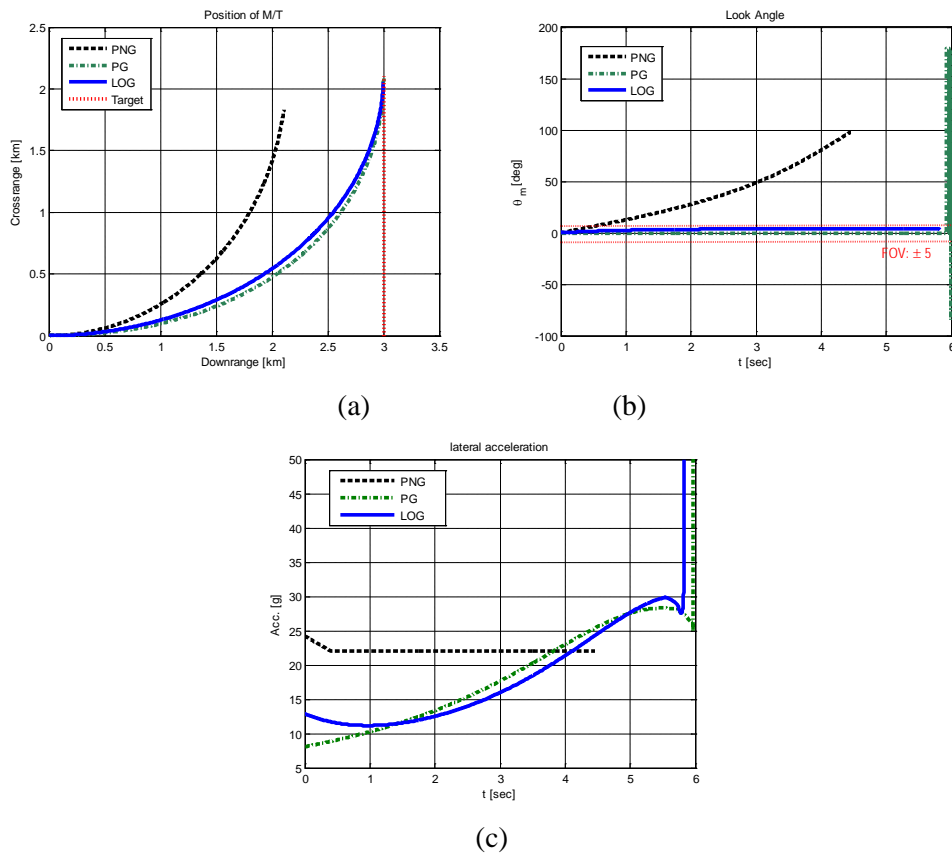
Figure 4.8: Simulation results of PNG, PG, and LOG law under conditions shown in Table 4.7. (a) position trajectories of missiles guided by several guidance laws and a target, (b) look angles of the missile, and (c) lateral accelerations of a missile. In the case of ideal autopilot dynamics, (c) presents both lateral and command lateral acceleration because both accelerations are the same. (Case I: Ideal autopilot dynamics.)

(a)

(b)

(c)
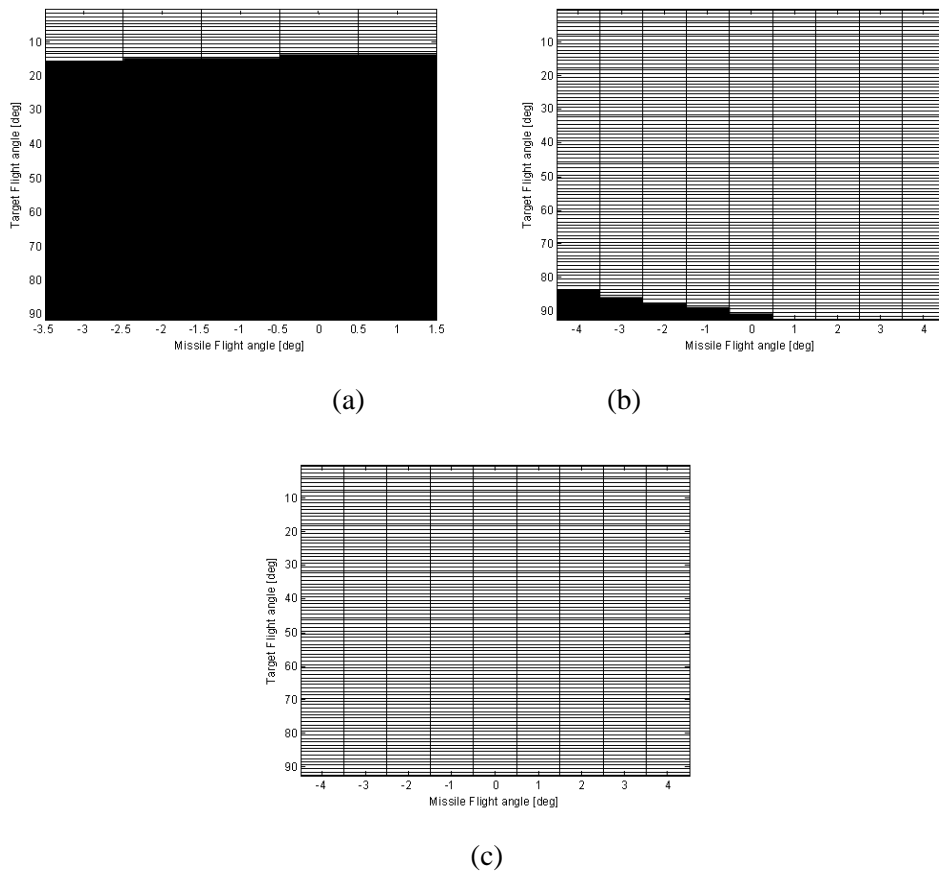
Figure 4.9: Whether or not lock-on condition is maintained in the cases of (a) PNG, (b) PG, and (c) LOG laws. These simulation results were obtained under the conditions shown in Table 4.8. The white areas show where a missile maintains the lock-on condition during the entire guidance time. The black areas show where the missile fails to maintain lock-on condition during the entire guidance time. (Case I: Ideal autopilot dynamics.)

(a)   (b)

(c)

Figure 4.10: Miss distance in the cases of (a) PNG, (b) PG, and (c) LOG laws. These simulation results were obtained under the conditions shown in Table 4.8. (Case I: Ideal autopilot dynamics.)

Case II: First Order Autopilot Dynamics

We analyzed the guidance performance assuming that the autopilot of the missile has first order dynamics. The simulation is carried out under the same condition as described in Table 4.7, except for first order autopilot dynamics. First, in order to show the position trajectory of the missile and the target, and the look angle of the missile, we performed a simulation with the spec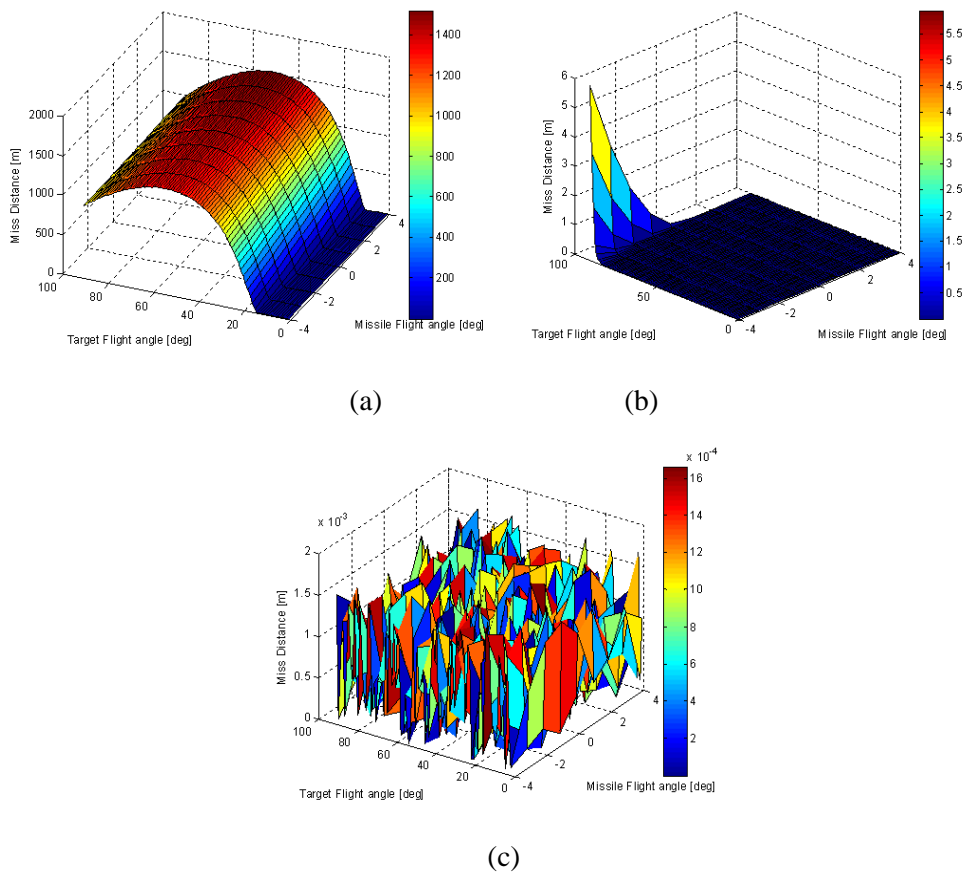ific engagement geometry shown in Table 4.9. Fig 4.11 presents the simulation result under the engagement geometry given in Table 4.9. It can be seen that the missile guided by both the PNG and the PG law failed the mission of intercepting the target (Fig 4.11(a)) because the target escaped the bound of the strapdown seeker's FOV. Even though the lock-on condition was broken almost near the target, the missile guided by the LOG law completed an excellent intercept mission. The miss distances of the PNG, PG, and LOG laws are 887.84 [m], 926.23 [m], and 1.36 [m], respectively. The capture region is presented in Fig 4.12. This simulation result was obtained under the conditions shown in Table 4.10. The white areas show that the miss distance of the missile and target is within 2 [m]; that is, the missile captured the target. The black areas indicate that the miss distance of the missile and target is over 2 [m]. It can be seen that the capturability performance of the LOG law is superior to that of the other guidance laws shown in Fig. 4.12. The miss distances for several cases of engagements are depicted in Fig 4.13. When the initial flight angle of the target is smaller than 10 [deg], the miss distances of the PNG law are

short because the look angle does not deviate from the FOV limit, even when using the

PNG law. However, as the initial flight angle of the target increases more than 10 [deg],

the miss distance increases exponentially. We can also see that for the PG law, the

interception performance decreased and the missile failed to intercept the target in

many given engagement conditions. On the other hand, with the LOG law, interception

of the target was accomplished under the given engagement conditions, even though

the miss distance slightly increased.

Table 4.9: Engagement parameters and geometry for evaluation of LOG law against nonmaneuvering target at high speed (Case II: first order autopilot dynamics.)

	Missile	Target
FOV	±5 [deg]	-
Initial velocity	680 [m/s]	350[m/s]
Initial relative position	(0,0) [m]	(3000,0)[m]
Initial orientation	0 [deg]	89 [deg]
Lateral acceleration limit	50g	-
Time constant	0.5 (sec)	-

Table 4.10: Engagement parameters and various geometries for evaluation of LOG law law against nonmaneuvering target at high speed (Case II: first order autopilot dynamics)

	Missile	Target
FOV	±5 [deg]	-
Initial velocity	680 [m/s]	350 [m/s]
Initial relative position	(0,0) [m]	(3000,0) [m]
Initial orientation	-4:1:4 [deg]	0:1:90 [deg]
Lateral acceleration limit	50g	-
Time constant	0.5 (sec)	-

(a)

(b)

(c)   (d)   (e)
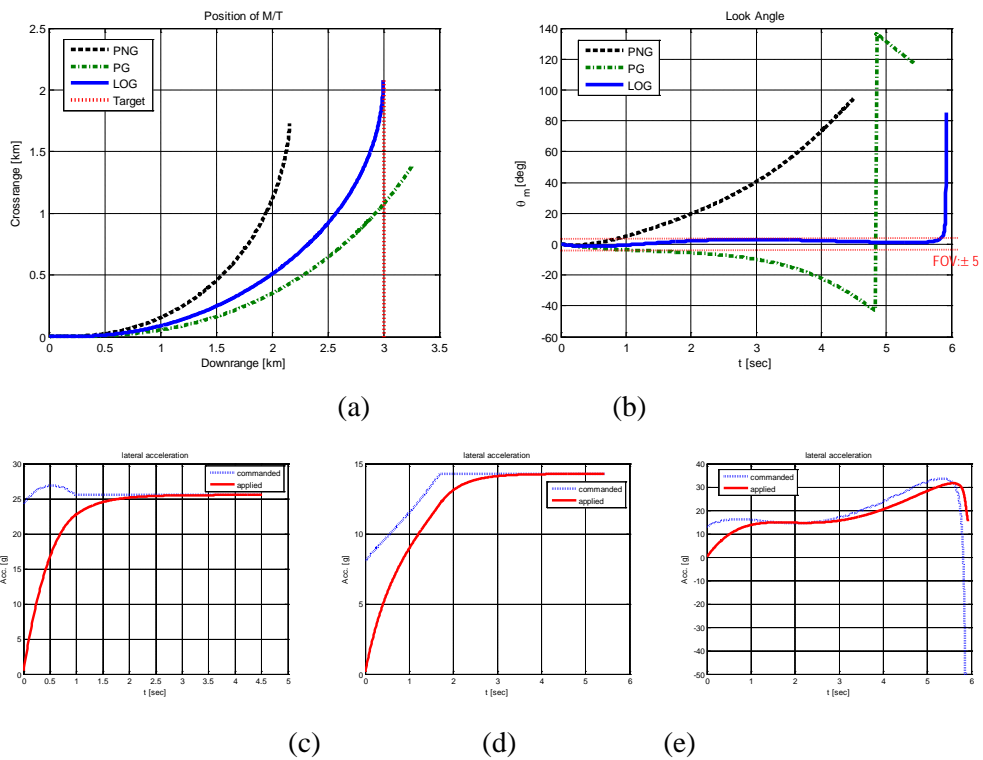
Figure 4.11: Simulation results of PNG, PG, and LOG law under conditions shown in Table 4.9. (a) shows position trajectories of missiles guided by several guidance laws and a target and (b) shows look angles of the missile. (c), (d), and (e) show the commanded and applied lateral accelerations in the case of the missile guided by PNG, PG, and proposed LOG law, respectively. (Case II: first order autopilot dynamics.)

(a)   (b)

(c)
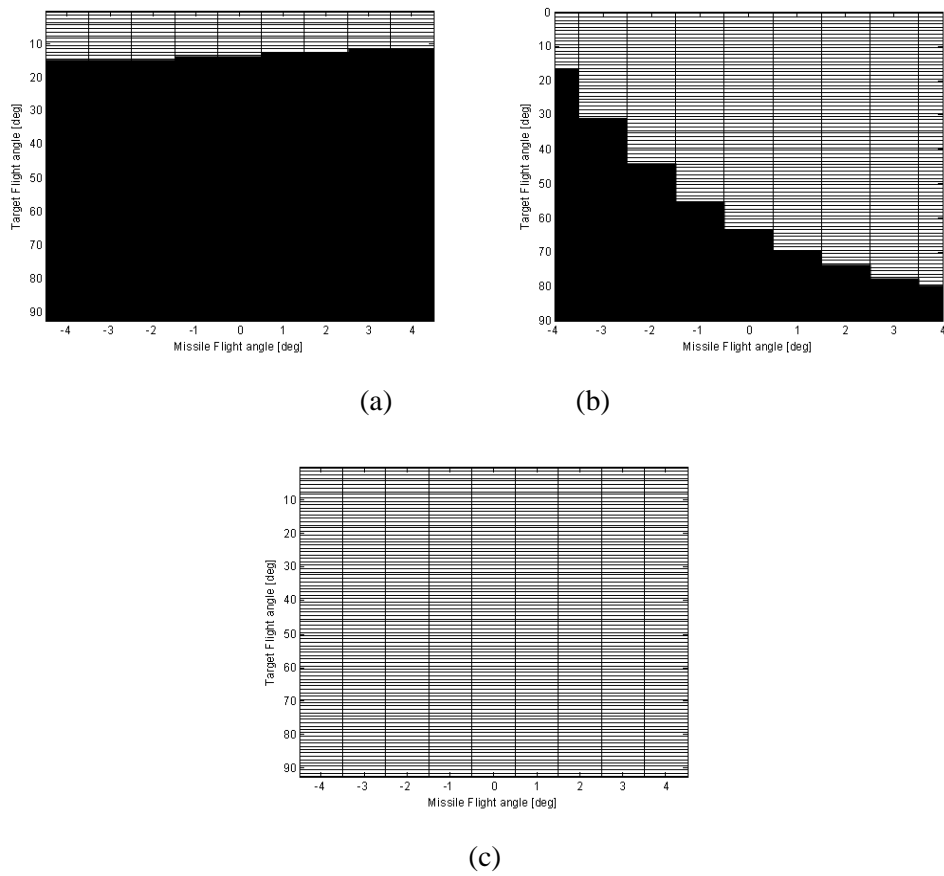
Figure 4.12: Capture region of (a) PNG, (b) PG, and (c) LOG law under the conditions shown in Table 4.10. The white areas show where the miss distance is within 2 [m] and the black areas show where the miss distance is over 2 [m]. (Case II: First order autopilot dynamics.)

(a)   (b)

(c)

Figure 4.13: Miss distances of (a) PNG, (b) HG, and (c) LOG laws under conditions shown in Table 4.10. (Case II: First order autopilot dynamics.)

4.2.2 **Maneuvering Target**

To evaluate the potential of the proposed LOG law against a maneuvering target, a performance evaluation is carried out using a simulation for the low (2g) and medium (6g) maneuvering targets. The series of processes of simulation is identical to that of the simulation for the HG law discussed in chapter 4.1.2. The simulation results for a high (8g) maneuvering target are omi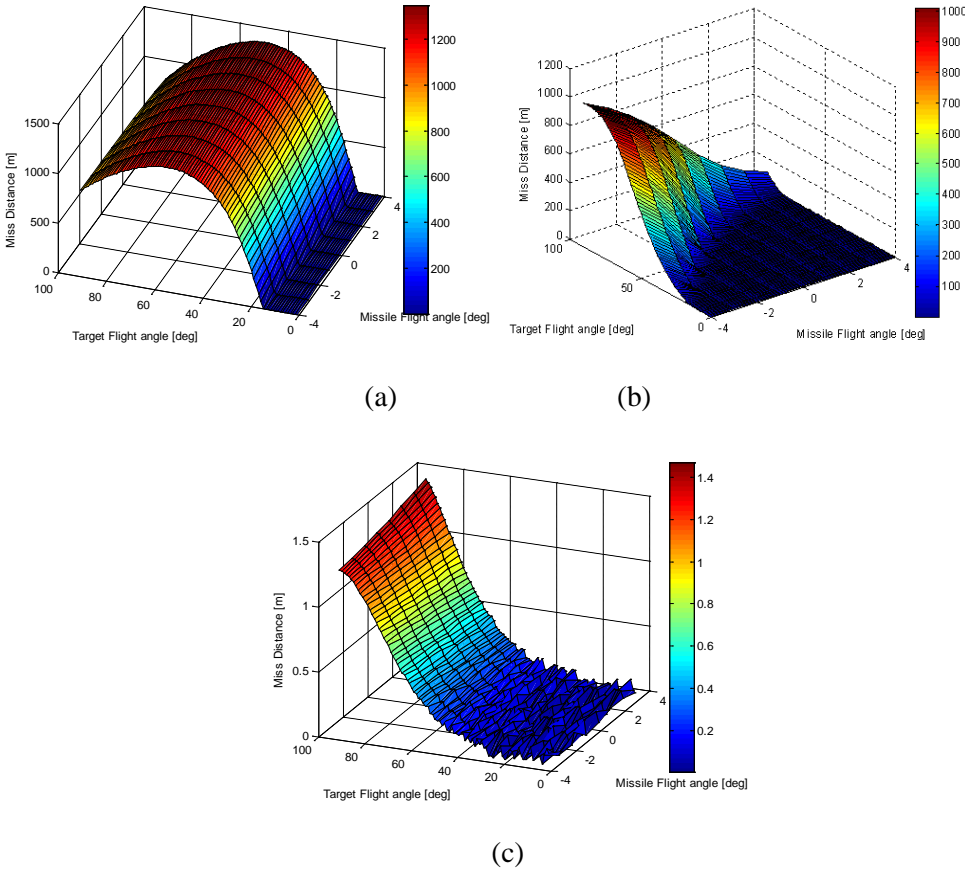tted in this dissertation since other simulation results are sufficient to evaluate and analyze the guidance performance of the proposed LOG law against a maneuvering target.

Low Maneuvering Target

Table 4.11 and Table 4.12 list the engagement parameters and geometry for evaluation of the LOG law against a low maneuvering target. The two tables list the same engagement parameters, except the time histories of the target acceleration. The scenarios of the target maneuver are identical to those described in section 4.1.2. In addition, the limit of the FOV of the strapdown seeker is ±5 [deg]. Fig 4.14 and Fig 4.15 presents simulation results of the PNG, the PG, and the LOG laws under the conditions listed in Table 4.11 and Table 4.12, respectively. The missiles guided by the PNG law miss the target soon after launching, while those guided by the PG law miss the target at about 5 [sec], and thus fail interception. However, as shown in Fig 4.14, the missile guided by the LOG law maintains the lock-on condition until interception

and successfully completes the engagement with a miss distance of 1.71 [m]. However, in another maneuvering target scenario as given in Table 4.12, the missile employing the LOG law fails the engagement, with a miss distance of 9.88 [m]. This guidance performance is thus not satisfactory. Since it has the first order autopilot dynamics, the missile cannot follow the target when the target lying near the FOV limit of the missile attempts to maneuver towards the direction of escape as shown in Fig 4.15.

Table 4.11: Engagement parameters and geometry for evaluation of LOG law against low maneuvering target, $-2g(0 < t < 2)$, $0g(2 < t < 3)$, $2g(3 < t)$
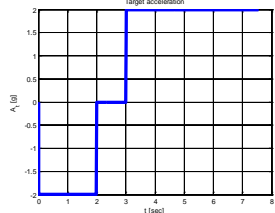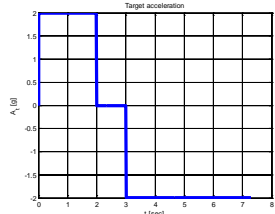
	Missile	Target
FOV	±5 [deg]	-
Initial velocity	680 [m/s]	350[m/s]
Initial relative position	(0,0) [m]	(3000,0)[m]
Initial orientation	0 [deg]	60 [deg]
Lateral acceleration limit	50g	-
Time constant	0.5 (sec)	-
Maneuver	-	

Table 4.12: Engagement parameters and geometry for evaluation of LOG law against low maneuvering target, $2g(0 < t < 2)$, $0g(2 < t < 3)$, $-2g(3 < t)$

	Missile	Target
FOV	±5 [deg]	-
Initial velocity	680 [m/s]	350[m/s]
Initial relative position	(0,0) [m]	(3000,0)[m]
Initial orientation	0 [deg]	60 [deg]
Lateral acceleration limit	50g	-
Time constant	0.5 (sec)	-
Maneuver	-	

Figure 4.14: Simulation results of PNG, PG, and LOG law under conditions shown in Table 4.11. (a) shows position trajectories of missiles guided by several guidance laws and a target and (b) shows the look angles of the missile. (c), (d), and (e) show the commanded and applied lateral accelerations in the case of the missile guided by the PNG, PG, and proposed LOG law, respectively. The missiles guided by the PNG, PG, and LOG laws miss the target at about 1 [sec], 5 [sec], and directly before interception, respectively. The miss distances in the cases of the PNG, PG, and LOG laws are about 1297 [m], 92 [m], and 1.71 [m], respectively.

(a)   (b)

(c)   (d)   (e)

Figure 4.15: Simulation results of PNG, PG, and LOG laws under conditions shown in Table 4.12. (a) shows position trajectories of missiles guided by several guidance laws and a target and (b) shows look angles of the missile. (c), (d), and (e) show the commanded and applied lateral accelerations in the case of the missile guided by the PNG, PG, and proposed LOG laws, respectively. The missiles guided by the PNG, PG, and LOG laws miss at about 1 [sec], 4 [sec], and 6.5 [sec] (which is directly before interception), respectively. All guidance laws fail to intercept.

Medium Maneuvering Target

Table 4.13 (Table 4.14) lists the engagement parameters and geometry for the evaluation of HG law against a medium maneuvering target, where the target initiates a $-6g$ ($6g$) dive turn at the beginning of interception, switches to a level flight after 2 [sec], and then executes a $6g$ ($-6g$) evasive maneuver after 1 second and continues until interception. Fig 4.16 (Fig 4.17) presents the simulation results of the PNG, the PG, and the LOG laws under the conditions listed in Table 4.13 (Table 4.14). All simulated guidance laws fail the engagement. In the case where the missile has a seeker with an extremely narrow FOV (± 5 [deg]), it is impossible for the missile to intercept the target with more than a medium maneuver, regardless of the guidance law adopted.

Table 4.13: Engagement parameters and geometry for evaluation of LOG law against medium maneuvering target, $-6g(0 < t < 2),\ 0g(2 < t < 3),\ 6g(3 < t)$
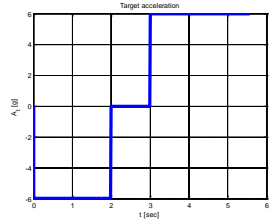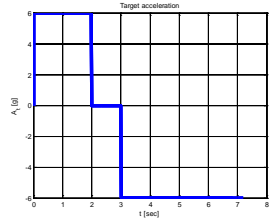
	Missile	Target
FOV	±5 [deg]	-
Initial velocity	680 [m/s]	350[m/s]
Initial relative position	(0,0) [m]	(3000,0)[m]
Initial orientation	0 [deg]	60 [deg]
Lateral acceleration limit	50g	-
Time constant	0.5 (sec)	-
Maneuver	-	

Table 4.14: Engagement parameters and geometry for evaluation of LOG law against medium maneuvering target, $6g(0 < t < 2),\ 0g(2 < t < 3),\ -6g(3 < t)$

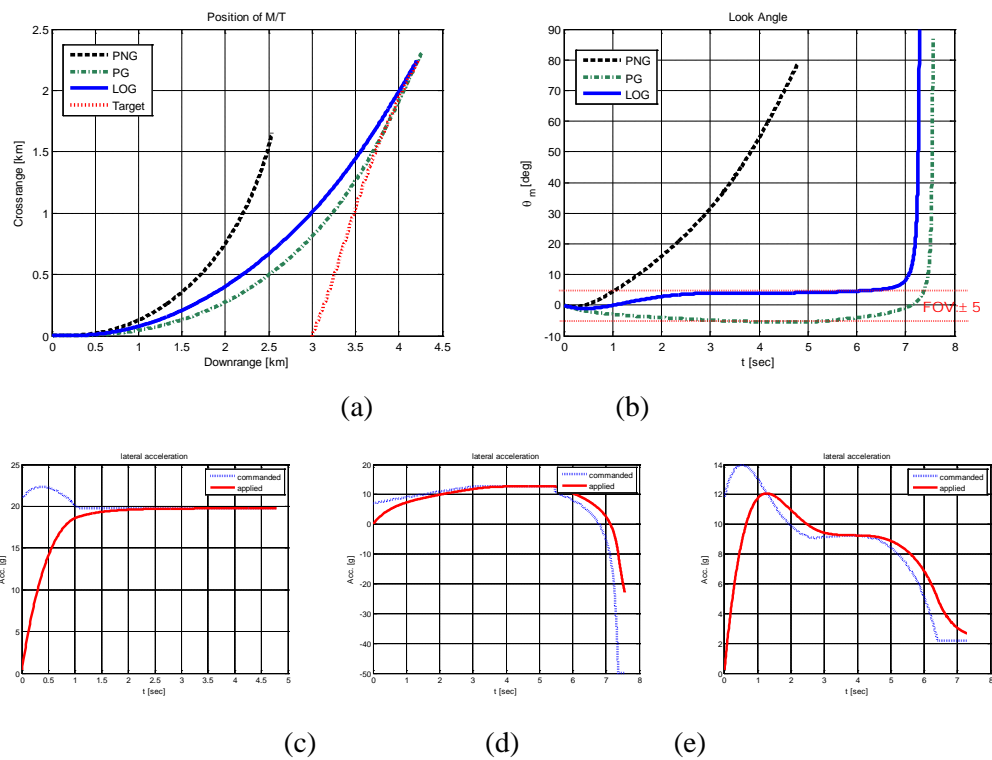|	Missile	Target
FOV	±5 [deg]	-
Initial velocity	680 [m/s]	350[m/s]
Initial relative position	(0,0) [m]	(3000,0)[m]
Initial orientation	0 [deg]	60 [deg]
Lateral acceleration limit	50g	-
Time constant	0.5 (sec)	-
Maneuver	-	

Figure 4.16: Simulation results of PNG, PG, and LOG laws under conditions shown in Table 4.13. (a) shows position trajectories of missiles guided by several guidance laws and a target and (b) shows look angles of the missile. (c), (d), and (e) show commanded and applied lateral accelerations in the case of a missile guided by PNG, PG, and the proposed LOG laws, respectively. The missiles guided by the PNG, PG, and LOG laws miss the target at about 1 [sec], 5 [sec], and a time immediately before the intercept, respectively. The miss distances in the case of the PNG, PG, and LOG laws are about 1325 [m], 269 [m], and 10.90 [m], respectively.

(a)   (b)

(c)   (d)   (e)
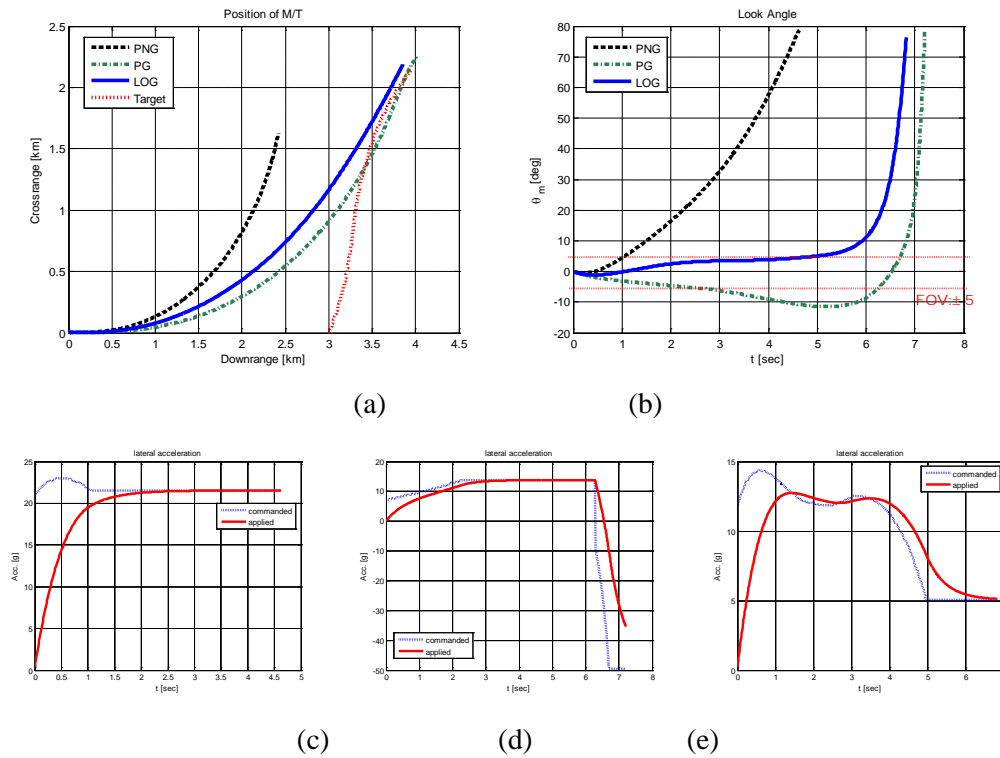
Figure 4.17: Simulation results of PNG, PG, and LOG laws under the conditions shown in Table 4.14. (a) shows position trajectories of missiles guided by several guidance laws and a target and (b) shows look angles of the missile. (c), (d), and (e) show commanded and applied lateral accelerations in the case of a missile guided by the PNG, PG, and proposed LOG laws, respectively. The missiles guided by the PNG, PG, and LOG laws miss the target at about 1[sec], 2.2[sec], and 5[sec], respectively. The miss distances in the cases of the PNG, PG, and LOG laws are about 1077 [m], 47 [m], and 105.65[m], respectively.

4.3 **Comparison of Hybrid Guidance Law and Lock-on Guidance Law**

In this subsection, we will compare two proposed guidance laws by analyzing their simulation results. ***Ed: highlight – please check if this should be 'subsection'.*** The performance criteria are as follows: capturability, tolerance of missile's initial flight angle error of the missile, and intercept time. Performance criteria are compared in the same engagement, except in the FOV range (HG: ±15 [deg], LOG: ±5 [deg]) as summarized in Table 4.15.

Capturability

Fig 4.18 presents the miss distance of the two proposed guidance laws when the missile's initial flight angle scopes are arranged equally at ±4 [deg]. The LOG law has considerably better capturability - even slight difference, provided the missile appears within the sight of the target. Allowing for the narrower strapdown seeker's FOV of the missile guided by the LOG law, the LOG law is expected to have better intercept performance in the actual engagement.

Tolerance of Missile's Initial Flight Angle Error

Fig 4.19(a) and Fig 4.19(b) represent the capture region obtained in the conditions shown in Table 4.2 and Table 4.8, respectively. Because the HG law is suitable for a

relatively wider strapdown seeker, the perceptible range of the seeker is larger and a greater initial flight angle error of the missile is allowed. In detail, the missile guided by the HG law can capture the target when launched initially at an angle from about -5 [deg] to 15 [deg], while the missile guided by the LOG law can intercept the target when launched from about -5 [deg] to 5 [deg].

Intercept Time

Analyzing the intercept time according to the condition given in Table 4.15, the missile guided by the HG law has a considerably shorter intercept time than the LOG law, as shown in Fig 4.20(a). This is because the HG law attempts to guide the missile to the expected position at which it will intercept the target in the future, while the LOG law guides the missile to be slightly ahead of the target as shown in Fig 4.20(b).

Table 4.15: Engagement parameters and various geometries for comparison of the HG law and the LOG law

	Missile	Target
FOV	HG: ±15 [deg] LOG: ±5 [deg]	-
Initial velocity	680 [m/s]	350 [m/s]
Initial relative position	(0,0) [m]	(3000,0) [m]
Initial orientation	-4:1:4 [deg]	0:1:90 [deg]
Lateral acceleration limit	50g	-
Time constant	0.5 (sec)	-

(a)   (b)
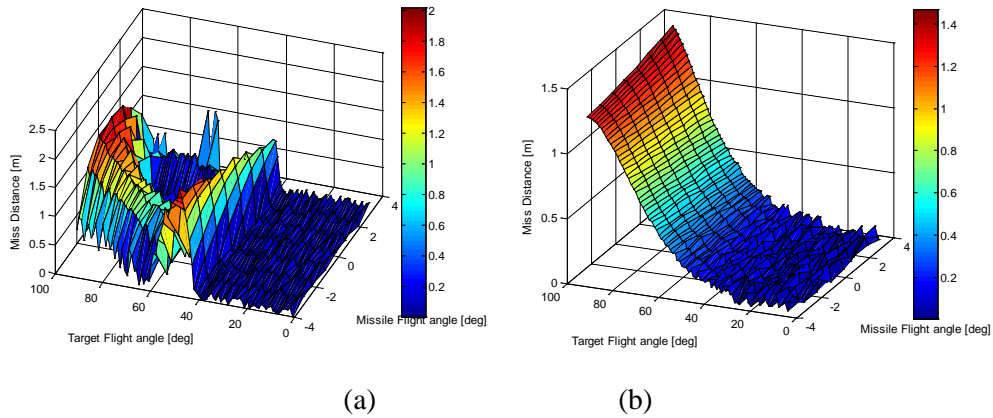
Figure 4.18: Miss distances of (a) HG and (b) LOG laws in the case of initial flight angle of a missile at ±4 [deg] under conditions shown in Table 4.15.

(a)   (b)
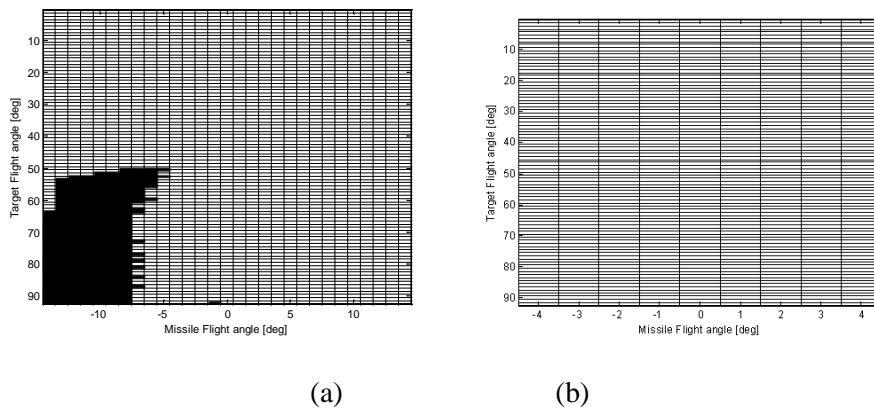
Figure 4.19: Capture regions of (a) HG and (c) LOG laws under conditions shown in Table 4.2 and Table 4.8, respectively. The horizontal axis of (a) ranges from -14[deg] to 14[deg] and that of (b) ranges from -4 [deg] to 4 [deg].

(a)   (b)
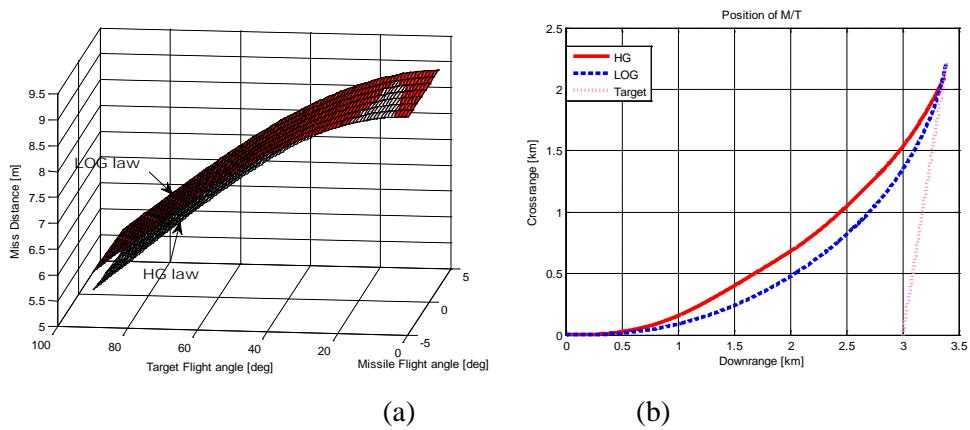
Figure 4.20: (a) shows intercept times of the HG and LOG laws under conditions shown in Table 4.15. (b) shows the reason for the difference of intercept time between the HG and LOG laws.

Chapter 5

Conclusions

5.1 Concluding Remarks

We have proposed a hybrid guidance (HG) law that is suitable for strapdown seekers with a narrow FOV (e.g. ± 15 [deg]) against a high-speed target. The PNG law was used to null the LOS rate to the target as the first guidance law, mixed with a guidance law to lessen the look angle as the second guidance law. We used the sliding mode control methodology to derive the second guidance law. In addition, to improve the guidance performance, we determined the switching boundary between the first and second guidance laws in real time. The switching boundary was selected to use the PNG law as much as possible during the overall homing phase. In addition, improvement was achieved in that the FOV of the strapdown seeker is widened somewhat by this modified guidance law. The proposed guidance law excellently accomplished interception of the target, whereas the conventional PNG law failed to intercept the target due to the narrow seeker FOV. We have also proposed another guidance law that is suitable for a strapdown seeker with a very narrow FOV (e.g. ± 5 [deg]) against a high-speed target, called the lock-on guidance (LOG) law. Because the accuracy of the measurement of the target is inversely proportional to the FOV, the seeker is often implemented with a very narrow FOV in order to improve the

measurement accuracy. The LOG law is applicable to this kind of seeker. The concept

of the LOG law is to make the edge of the FOV align with the target. By doing this, the

missile achieved a larger effective FOV than it actually has. Furthermore, since the

missile moves toward the future location of the target, this guidance law improves

upon a weak point of the pursuit guidance law. The LOG law was derived by

employing a Lyapunov-like function with the sliding-mode control methodology. In

order to verify the proposed guidance law, a simulation was carried out for various

engagements. The LOG law demonstrated superior guidance performance compared to

conventional PNG law and PG law for a narrow FOV.

The LOG law is superior to the HG law in terms of miss distance for a strapdown

seeker which has a very narrow FOV, and in terms of its excellent measurement

accuracy. For a missile using a strapdown seeker with a very narrow FOV, the guidance

performance of the HG law is not satisfactory. In contrast, the guidance performance of

the LOG law is not good when the FOV of the strapdown seeker is relatively large. The

HG law is superior to the LOG law in terms of intercept time. The HG law is also more

generous to initial heading error than the LOG law, since it can be applied to guidance

using a strapdown seeker with a larger FOV.

The proposed guidance laws have better performance than the conventional

guidance laws for a missile equipped with a strapdown seeker. Due to the natural

limitations of a strapdown seeker, there are some constraints to apply the proposed

guidance laws to an actual guidance system.

5.2 Further Study

In order to apply the proposed guidance laws to a tactical missile, a number of issues remain to be investigated. First, the switching boundary estimation in the HG law is calculated under the assumption that an estimated value of the LOS angular rate and an actual LOS angular rate at the time of estimation are the same for simplicity of calculation. This assumption causes somewhat inaccurate estimation. In order to obtain a more accurate estimation, the estimated value of the LOS angular rate will have to be calculated without this assumption. Second, the HG law does not consider the maneuvering of the target in the switching boundary estimator. Thus, the proposed HG law is vulnerable to a maneuvering target. Additional information about the maneuvering target will reinforce the guidance performance of the proposed HG law. The rest of the drawbacks of the proposed guidance laws come from hardware limitations such as an extremely narrow FOV, limited measurement, the dynamics of the missile, and so on. Continuous improvements of the proposed guidance laws will undoubtedly enable the guidance law for strapdown seekers to take major steps forward.

Bibliography

[1]   Z. Paul, "Tactical and Strategic Missile Guidance, Third Edition," Progress in Astronautics and Aeronautics, Vol. 176, 1997.

[2]   A. S. Locke, "Guidance," D. Van Nostrand Co., Princeton, 1955.

[3]   R. M. Howe, "Guidance," System Engineering Handbook, McGraw-Hill, New York, 1965.

[4]   L. Teng and P. L. Phipps, "Application of Nonlinear Filter to Short Range Missile Guidance," Proceedings, Journal of Astrpnautical Sciences, June 1968, pp. 138-147.

[5]   R. W. Rishel, "Optimal Terminal Guidance of An Air to Surface Missile," Paper No. 67-580, AIAA Guidance, Control and Flight Dynamics Conference, Aug. 1967.

[6]   R. Goodstein, "Guidance Law Applicability to Missile Closing," Guidance and Control of Tactical Missiles, AGARD Rept. LS-52, May 1972.

[7]   J. Clemow, "Missile Guidance," Temple Press Unlimited, London, 1960

[8]   G. L. Harmon, K.E. Kent, and W.P. Purcell, "Optimal Bang-Bang Guidance System," Paper 19.1, Western Electric Show and Convention, Part. 5, 1962.

[9]   R. Thibodeau and J. B. Sharp, "PDM Control Analysis Using the Phase Plane," Journal of Spacecraft and Rockets, pp. 1054-1057, 1969.

[10] A. Ivanov, "Radar Guidance of Missiles," Proceedings of IEEE International Conference, pp. 321-335, 1975.

[11] J. E. Kain and D. J. Yost, "Command to Line-of-Sight Guidance: A Stochastic Optimal Control Problem," AIAA Guidance and Control Conference Proceedings, pp. 356-364, 1976.

[12] H. Spits, "Partial Navigation Courses for a Guided Missile Attacking a Constant Velocity Target," Naval Research Laboratory, Washington, D.C., Rept. R-2790, 1946.

[13] L. A. Irish, "A Basic Control Equation for Rendezvous Terminal Guidance," IRE Transactions Aerospace and Navigational Electronics, pp. 106-113, 1961.

[14] B. A. McElhoe, "Minimal-Fuel Steering for Rendezvous Homing Using Proportional Navigation," American Rocket Society Journal, pp. 1614-1615, 1962.

[15] T. W. J. Wong, "Guidance Systems for Air-to-Air Missiles," Interavia, pp. 1525-1528, 1961.

[16] M. Guelman, "The Closed-Form Solution of True Proportional Navigation," IEEE Transactions on Aerospace and Electronic systems, Vol. aes-12, No. 4, pp. 472-482, 1976.

[17] M. Guelman, "Proportional navigation with a maneuvering target," IEEE Transactions on Aerospace and Electronic Systems, Vol. AES-8, 364-371, 1972.

[18] I. J. Ha, J. S. Hur, M. S. Ko, and T. L. Song, "Performance analysis of PNG laws for randomly maneuvering targets," IEEE Transactions on Aerospace and Electronic Systems, Vol. 26, 713-721, 1990.

[19] D. Ghose, "True Proportional Navigation With Maneuvering Target," IEEE Transactions on Aerospace and Electronic systems, Vol. 30, No. 1, pp. 229-237, 1994.

[20] D. Ghose, "On the Generalization of True Proportional Navigation," IEEE Transactions on Aerospace and Electronic Systems , Vol. AES-30, pp. 545 – 555, 1994.

[21] P. J. Yuan and J. S. Chern, "Ideal Proportional Navigation," Journal of Guidance, Control, and Dynamics, Vol. 15, No. 5, pp. 1161-1166, 1992.

[22] A. E. Jr. Bryson, W. F. Denham and S. E. Dreyfus, "Optimal Programming Problems with Inequality Constraints I: Necessary Conditions for External Solutions," AIAA Journal, pp. 2544-2550, 1963.

[23] W. F. Denham, and A. W. Jr. Bryson, "Optimal Programming Problems with Inequality Constraints II: Solution by Steepest Descent," AIAA Journal, pp. 25-34, 1964.

[24] W. F. Denham, "Range Maximization of a Surface-to-Surface Missile with In-Flight Inequality Constraints," Journal of Spacecraft and Rockets, pp. 78-83, 1964.

[25] E. R. Rang, "A Comment on Closed-Loop Optimal Guidance Systems," IEEE Transactions on Automatic Control, pp. 616-617, 1966.

[26] R. W. Rishel, "Optimal Terminal Guidance of An Air to Surface Missile," Paper No. 67-580, AIAA Guidance, Control and Flight Dynamics Conference, 1967.

[27] E. I. Axelband and F.W. Hardy, "Quasi-Optimum Proportional Navigation," 2nd Hawaii International Conference System Sciences, pp. 417-421, 1969.

[28] E. I. Axelband and F.W. Hardy, "Optimal Feedback Missile Guidance," 3rd Hawaii International Conference System Sciences, pp. 874-877, 1970.

[29] G. M. Anderson, "A Near Optimal Closed-Loop Solution Method for Nonsingular Zero-Sum Differential Games," Journal of Optimization Theory and Applications, Vol. 13, No. 3, pp. 303-318, 1974.

[30] R. A. Poulter and G.M. Anderson, "A Guidance Concept for Air-to-Air Missiles Based on Nonlinear Differential Game Theory," National Aerospace Electronics Conference, pp. 605-609, 1976.

[31] N. K. Gupta and B. Sridhar, "Reachable Sets for Missile Guidance against Smart Targets," Proceedings of the National Aerospace and Electronics Conference, pp. 780-787, 1979.

[32] S. Gutman, "On Optimal Guidance for Homing Missiles," Journal of Guidance and Control, pp. 296-300, 1979.

[33] R. A. Best and J. P. Norton, "Predictive Missile Guidance," Journal of Guidance, Control, and Dynamics, Vol. 23, No. 3, pp. 539-546, 2000.

[34] D. Dionne, H. Michalska and C. A. Rabbath, "A Predictive Guidance Law with uncertain information about the Target State," pp. 1062-1067, 2006.

[35] K. R. Babu, I. G. Sarma and K. N. Swamy, "Switched Bias Proportional Navigation for Homing Guidance Against Highly Maneuvering Targets," Journal of Guidance, Control and Dynamics, Vol. 17, No. 6, pp. 1357-1363, 1994.

[36] D. Zhou, C. Mu and W. Xu, "Adaptive Sliding-Mode Guidance of a Homing Missile," Journal of Guidance, Control and Dynamics, Vol. 22, No. 4, pp. 589-594, 1999.

[37] J. Moon, K. Kim and Y. Kim, "Design of Missile Guidance Law via Variable Structure Control," Journal of Guidance, Control and Dynamics, Vol. 24, No. 4, pp. 659-664, 2001

[38] R. K. Mehra and R. D. Ehrich, "Air-to-Air Missile Guidance for Strapdown Seekers," Proceedings of 23rd Conference on Decision and Control, pp. 1109-1115, 1984.

[39] J. S. Yun, C.K. Ryoo and T.L. Song, "Strapdown Sensors and Seeker Based Guidance Filter Design," International Conference on Control Automation and Systems, pp. 468-472, 2008.

[40] D. W. Kim, C. K. Ryoo, Y. H. Kim and J. J Kim, "Guidance and Control for Missiles with a Stradown Seeker," 11th International Conference on Control Automation and Systems, pp. 969-972, 2011.

[41] S. A. Jang, C.K. Ryoo, K. Y Choi and M. J. Tahk, "Guidance Algorithms for Tactical Missiles with Strapdown Seeker," SICE Annual Conference, pp. 2616-2619, 2008

[42] Y. L. Du, Q. L. Xia and T. Guo, "Study on Stability of Strapdown Seeker Scale Factor Error Parasitical Loop," International Conference on Computer, Mechatronics, Control and Electronic Engineering, pp. 55-58, 2010.

[43] 오승민, "스트랩다운 탐색기를 장착한 전술유도탄의 UKF 기반 종말호밍 유도," 한국항공우주학회지, pp. 221-227, 2010.

[44] 장세아, 유창경, 최기영, 탁민제, "스트랩다운 탐색기를 탑재한 휴대용 전술유도무기 유도루프 설계," 항공우주학회 춘계학술, pp. 319-322, 2008.

[45] 장세아, 유창경, 최기영, "스트랩다운 탐색기를 탑재한 유도탄의 Parasite Loop 보상," 제15차 유도무기 학술대회, pp. 65-70, 2009.

[46] 윤중섭, 유창경, 송택렬, "스트랩다운 탐색기 및 MEMS 센서를 이용한 유도필터 설계," 한국항공우주학회지, pp. 1002-1009, 2009

[47] 김태훈, 박봉균, 권혁훈, 김윤환, 탁민제, "스트랩다운 탐색기를 탑재한 유도탄의 안정성 해석," 한국항공우주학회지, pp. 332-340, 2011.

[48]   L. Martina, P. Emidio and L. Sauro, "EKF application on estimating missile guidance signals," Communications to SIMAI Congress, Vol. 3, 2009.

[49]   G. J. Zhang, Y. Yao and K. M. Ma, "Line of Sight Rate Estimation of Strapdown imaging guidance system based on unscented kalman filter," Machine Learning and Cybernetics Conference, pp. 1574-1578, 2005.

[50]   Y. C. Zhang, J. J. Li and H. Y. Li, "Line of Sight Rate Estimation of Strapdown Imaging Seeker Based on Particle Filter," Machine Learning and Cybernetics Conference, pp. 1574-1578, 2005.

[51]   M. Xin, S. N. Balakrishnan, E. J. Ohlmeyer, "Guidance Law Design for Missiles with Reduced Seeker Field-of-View," AIAA Guidance, Navigation, and Control Conference and Exhibit, pp. 711-719, 2006.

[52]   D. K. Sang, C. k. Ryoo, M. J. Tahk, "A Guidance Law with a Switching Logic for Maintaining Seeker's Lock-on for Stationary Targets," KSAS International Journal. Vol. 9, No. 2, pp. 87-97, 2008.

[53]   P. Cheng, "A Short Survey on Pursuit-Evasion Games," Proceeding of Department of Computer Science, University of Illinois at Urbana-Champaign, 2003.

[54]   C. F. Lin, "Advanced Control Systems Design," Prentice Hall Series in Advanced Navigation, Guidance and Control and Their Applications, Prentice-Hall Inc., 1994.

[55] S. L. Ménec, "Extensive Comparison between Quantitative Pursuit Evasion Game Guidance Law and PNS," Proceedings 16th IFAC Symposium on Automatic Control in Aerospace, Saint-Petersburg, Russia, Vol. 2, pp. 51-55, June 14-18, 2004.

[56] P. Gurfil, M. Jodorkovsky and M. Guelman, "Neoclassical Guidance for Homing Missiles," Journal of Guidance, Control and Dynamics, Vol. 24, No. 3, pp. 452-459, 2001.

[57] J. Shinar and T. Shima, "Nonorthodox Guidance Law Development Approach for Intercepting Maneuvering Targets," Journal of Guidance, Vol. 25, No. 4, pp. 658-666, 2002.

[58] M. Siouris, "Missile Guidance and Control Systems," Springer Press, 2004.

[59] R. Yanushevsky, "Modern Missile Guidance," CRC Press, 2007.

[60] G. Wheeler, C.Y. Su and Y.R. Stepanenko, "A Sliding Mode Controller with Improved Adaptation Laws for the Upper Bounds on the Norm of Uncertainties," Automatica, Vol. 34, No. 12, pp. 1657-1661, 1998.

[61] D. S. Yoo and M. J. Chung, "A Variable Structure Control with Simple Adaptation Laws for Upper Bounds on the Norm of the Uncertainties," IEEE transactions on Automatic control, Vol. 37, No. 6, pp. 860-865, 1992.

[62] A. W. Thomas and S. R. Hebertt, "Variable-Structure Control of Spacecraft Attitude Maneuvers," Journal of Guidance, Dynamics and Control, Vol. 11, No. 3, pp. 262-270, 1998.

[63] A. W. Thomas and J.H. Kim, "Bandwidth-Limited Robust Nonlinear Sliding Control of Pointing and Tracking Maneuvers," American Control Conference, pp. 1131-135, 1989

[64] D. J. Shin and J. H. Kim, "Robust Spacecraft Attitude Control Using Sliding Mode Control," American Institute of Aeronautics and Astronautics, pp. 1508-1518, 1998.

[65] A. K. Scott and D. H. Christopher, "Spacecraft Attitude Sliding Mode Controller using Reaction Wheels," AIAA/AAS Astrodynamics Specialist Conference and Exhibit, pp. 1-28, 2008.

[66] C. H. Lee, C. Hyun, J. G. Lee, J. Y. Choi and S. K. Sung, "A Hybrid Guidance Law for a Strapdowns Seeker to Maintain Lock-on Conditions against High Speed Targets," Journal of Electrical Engineering & Technology, Vol. 8, No. 1, pp. 190-196, 2013.

[67] V. L. Utkin, "Variable Structure Systems with Sliding Modes," IEEE Transactions on Automatic Control, Vol. AC-22, No. 2, pp. 212-222, 1977.

[68] R. A. DeCarlo, S. H. Zak and G. P. Mathews, "Variable Structure Control of Nonlinear Multivariable Systems: A Tutorial," Proceeding IEEE, Vol. 76, No.3, 1988.

[69] W. Perruquetti, J. P. Barbot, "Sliding Mode Control in Engineering," Marcel Dekker Press, pp. 20-46, 2002.

[70] H. Asada and J.J. E. Slotine, "Robot Analysis and Control," pp.140-157, 1986 .

[71] A. G. Bondarev, S. A. Bondarev, N. E. Kostyleva and V. I. Utkin, "Sliding Modes in Systems with Asymptotic State Observers," Automation and Remote Control, pp.679 -684 1985.

[72] K. D. Young and U. Ozgiiner, "Frequency Shaping Compensator Design for Sliding Mode," Sliding Mode Control, pp.1005 -1019, 1993.

[73] K. D. Young and S. Drakunov, "Sliding mode control with chattering reduction," Proceedings of the 1992 American Control Conference, pp.1291 -1292, 1992.

[74] W. C. Su , S. V. Drakunov, U. Ozgiinerand and K. D. Young, "Sliding mode with chattering reduction in sampled data systems," Proceedings of the 32nd IEEE Conference on Decision and Control, pp.2452 -2457, 1993.

[75] K. D. Young and S. V. Drakunov, "Discontinuous frequency shaping compensation for uncertain dynamic systems," Proceedings 12th IFAC World Congress, pp.39 -42, 1993.

[76] C. S. Shieh, "Tunable H∞ Robust Guidance Law for Homing Missiles," IEE Proceedings on Control Theory Applications, Vol. 151, No. 1, pp. 103-107, 2004.

[77] H. L. Pastrick and S. M. Seltzer, "Guidance Laws for Short-Range Tactical Missiles," Journal of Guidance and Control, Vol. 4, No. 2, pp. 98-108, 1981.

[78] B. Özkan, "Dynamic Modeling, Guidance and Control of Homing Missiles," PhD Thesis, Mechanical Engineering Department, Middle East Technical University, Turkey, 2005.

[79] P. L. Vergez and J. R. McClendon, "Optimal Control and Estimation for Strapdown Seeker Guidance of Tactical Missiles," Journal of Guidance, Control and Dynamics, Vol. 5, No. 3, 1982

국문초록

유도탄은 전투의 전술적인 목적에 따라 다양한 형태로 제작된다. 유도탄의 일회성으로 인해 저가의 유도탄 개발의 필요성이 대두되고 이의 일환으로 유도탄에 고가의 김블 탐색기를 대신해서 저가의 스트랩다운 탐색기를 사용하려는 연구가 진행되고 있다. 본 논문에서는 유도탄에 장착되는 탐색기로 김블 탐색기 대신 스트랩다운 탐색기로 대체할 경우에 발생 가능한 문제점을 해결하고자 하였다. 스트랩다운 탐색기는 김블 탐색기에 비해 장착 및 구현 비용이 적고, 김블 플랫폼을 제거함으로써 기계적 복잡성을 제거할 수 있으며 구현이 쉽다는 장점을 가진 반면에 작은 화각과 획득 가능한 정보가 제한적이라는 단점을 가지고 있다. 본 논문에서는 화각(field-of-view)이 작고 시야각 정보만을 측정할 수 있는 스트랩다운 탐색기를 이용하여 유도탄을 표적까지 유도를 수행할 때, 유도 성능과 안정성을 높이기 위한 기법을 제안하였으며 시뮬레이션을 통하여 제안한 기법의 성능을 검증하였다. .

먼저 구현의 용이함과 안정성 때문에 현재 널리 사용되고 있는 비례항법 유도법칙을 스트랩다운 탐색기를 장착한 유도탄에 적용할 경우에 탐색기의 작은 화각으로 인해 유도 중 표적을 잃는 경우가 발생한다. 또한 기존의 다른 유도법칙도 작은 화각과 제한된 정보로 인하여 유도 성능이 현저히 떨어진다. 이러한 문제를 해결하기 위한 방법으로 혼합유도기법을 제안하였다. 비례항법유도법칙을 주 유도법칙으로 사용하고 비례항법유도법칙으로 인해서 커진 시야각(look angle)을 줄이기 위한 유도법칙으로 슬라이딩 모드 제어를 이용하여 유도된 유도법칙을 사용하였다. 시야각이 일정 크기를 넘지 않은 경우에는 비례항법유도법칙을 사용하고 시야각이 특정 크기를 넘어설 경우에 본 논문에서 유도한 슬라이딩 모드 유도 법칙을 이용한다. 유도 성능

이 좋은 비례항법유도법칙을 최대한 사용하면서 표적이 시야각에서 벗어나지 않도록 하기 위하여, 두개의 유도 법칙이 스위칭되는 시야각의 특정 크기를 결정하는 연구도 수행하였다.

다음으로 스트랩다운 탐색기의 작은 화각으로 인해 발생하는 문제를 해결하는 또 다른 방법으로 락온유도기법을 제안하였다. 탐색기의 화각의 범위는 표적 측정 정밀도와 반비례한다. 즉, 화각이 작을수록 표적의 측정 정밀도가 높아진다. 측정 정밀도를 높이기 위해 유도탄에 장착되는 탐색기의 화각을 굉장히 작게 할 경우에도 유도가 가능하도록 하는 유도기법을 제안하였다. 락온유도기법은 추적유도기법의 개념을 기본으로 한다. 추적유도기법은 간단한 개념과 구현이 쉽다는 장점을 가지고 있지만 표적이 빠르게 기동하고 있을 경우 명중 성능이 현저하게 떨어진다. 락온 유도 기법은 추적유도기법의 단점을 보완하여 명중 성능을 높임으로써 기존유도기법을 스트랩다운 탐색기에 적용할 경우에 갖게 되는 한계를 극복할 수 있도록 하였다. 마지막으로 제안한 두 개의 유도 기법의 시뮬레이션 결과를 토대로 두 유도기법의 장단점을 비교하고 유도 성능을 분석하였다.

본 학위논문에서 제안된 방법들은 스트랩다운 탐색기의 단점 중에 하나인 좁은 화각 문제를 해결함으로써 저비용 유도탄 개발에 일조할 것으로 기대된다.

주요어: 스트랩다운 탐색기, 비례항법유도기법, 혼합유도기법, 추적유도기법, 락온유도기법

이 름: 이 채 흔
학 번: 2005-21485